
ERROR ANALYSIS OF AN HDG METHOD WITH IMPEDANCE TRACES FOR THE HELMHOLTZ EQUATION

Michael Leumüller

Institute of Analysis and Scientific Computing
TU Wien
Vienna, Austria

Joachim Schöberl

Institute of Analysis and Scientific Computing
TU Wien
Vienna, Austria

July 11, 2023

ABSTRACT

In this work, a novel analysis of a hybrid discontinuous Galerkin method for the Helmholtz equation is presented. It uses wavenumber, mesh size and polynomial degree independent stabilisation parameters leading to impedance traces between elements. With analysis techniques based on projection operators unique discrete solvability without a resolution condition and optimal convergence rates with respect to the mesh size are proven. The considered method is tailored towards enabling static condensation and the usage of iterative solvers.

MSC class: 65N12 (Primary) 65N30 (Secondary)

Keywords Helmholtz equation · hybrid discontinuous Galerkin method · finite elements · stability · convergence

1 Introduction

The numerical solution of the Helmholtz equation with impedance boundary conditions is challenging. For large wavenumbers the finite element method (FEM) yields, due to the necessary small mesh size, large systems of linear equations. The computational costs for direct solvers are too expensive and due to the indefinite structure of the Helmholtz equation, iterative solvers developed for elliptic problems cannot be applied. Domain decomposition preconditioners seem promising, but sub-blocks of finite element (FE) system matrices need to be inverted. For conforming FE spaces these blocks represent local Dirichlet problems which may be singular.

Discontinuous spaces can be applied to circumvent this issue leading to absolutely stable local methods, e.g. [FX13]. In [MPS13] a discontinuous Galerkin (DG) method for the Helmholtz equation has been proposed and analysed. It is remarkable that therein the existence of a discrete solution is proven without the need for a resolution condition of the discrete space. Quasi-optimality has been established in the asymptotic regime. Other studies of DG methods have been dedicated to giving explicit pre-asymptotic estimates, e.g. [FW09, FW11, FX13, Wu14]. The analysis is based on carefully chosen test functions contained in DG spaces. The same technique cannot be applied to conforming FE spaces.

A disadvantage of DG methods compared to standard FEM is the larger number of coupling unknowns. Hybrid discontinuous Galerkin (HDG) methods have been developed to counteract this issue. Applying static condensation leads to smaller systems of linear equations for skeleton unknowns. A requirement is the invertibility of element matrices which is closely related to local absolute stability. In [LCQ17] an absolutely stable HDG method for Maxwell's equations has been analysed via a new method based on L^2 -projections proving discrete absolute stability.

DG and HDG methods depend on stabilisations of jumps over facets, which usually are h -dependent stemming from the analysis of the elliptic Poisson equation. Contrary to that approach, the experiments in [Hub13, HPS13, HS14] suggests that iterative solvers for the Helmholtz equation require h -independent stabilisations representing impedance traces between sub-domains. In [GM11], an HDG method with such a stabilisation has been analysed. The used

technique is based on results from [CGS10] and utilises special projections tailored to the therein employed HDG formulation. The authors were able to prove optimal convergence rates in the asymptotic range.

The main contribution of this work is the analysis of the HDG formulation introduced in [MSS10] and further studied in [Hub13, HPS13, HS14]. The authors explored various promising iterative solvers, motivating the favourable properties of this HDG formulation. Numerical experiments therein suggest for solvers the necessity of a second variable per facet representing the flux, which is similar to the discontinuous Petrov Galerkin method in [DGMZ12, GMO14]. This work establishes the analytical foundation for the HDG method with two variables per facet introduced in [MSS10]. It utilises a mesh size, domain and wave number independent stabilisation which is a priori known for all Helmholtz problems. In Section 2, the HDG formulation is introduced and the main results, consisting of discrete absolute stability and optimal convergence rates, are stated. The consecutive sections are dedicated to proving these statements, starting with the discrete absolute stability in Section 3, followed by the optimal convergence for the pressure in Section 4 and of the flux in Section 5. In Section 6, simulations for problems with plane waves as analytical solutions are shown and to illustrate the potential of an iterative solver, a 2D example with heterogeneous materials and a 3D example with scattering objects are considered.

2 Hybrid Discontinuous Galerkin Method

This study considers the following mixed Helmholtz problem with an impedance boundary condition on a bounded Lipschitz domain $\Omega \subset \mathbb{R}^d$.

Definition 1 (Mixed Helmholtz Problem). For given $\kappa > 0$ and $g \in L^2(\partial\Omega)$, let (σ, u) be the solution of the boundary value problem (BVP)

$$j\kappa\sigma - \nabla u = 0 \quad \text{in } \Omega, \quad (1a)$$

$$-\operatorname{div} \sigma + j\kappa u = 0 \quad \text{in } \Omega, \quad (1b)$$

$$\sigma \cdot \mathbf{n} + u = g \quad \text{on } \partial\Omega. \quad (1c)$$

The outward pointing normal vector is denoted by \mathbf{n} , the imaginary unit is $j := \sqrt{-1}$, g represents a given excitation on $\partial\Omega$ and κ is a prescribed positive wavenumber. The flux and pressure are symbolised by σ and u . The corresponding adjoint problem is defined as follows.

Definition 2 (Adjoint Mixed Helmholtz Problem). For given $\kappa > 0$ and $f \in L^2(\Omega)$, let (ϕ, w) be the solution of the BVP

$$j\kappa\phi + \nabla w = 0 \quad \text{in } \Omega, \quad (2a)$$

$$\operatorname{div} \phi + j\kappa w = f \quad \text{in } \Omega, \quad (2b)$$

$$\phi \cdot \mathbf{n} + w = 0 \quad \text{on } \partial\Omega. \quad (2c)$$

The adjoint BVP has a homogenous Robin-boundary condition and a volume excitation f . The existence and uniqueness of the continuous BVPs have been proven in [Mel95, Proposition 8.1.3].

Remark 3. The mixed adjoint problem is equivalent to

$$-\Delta w - \kappa^2 w = j\kappa f \quad \text{in } \Omega, \quad (3a)$$

$$-\frac{1}{j\kappa} \nabla w \cdot \mathbf{n} + w = 0 \quad \text{on } \partial\Omega \quad (3b)$$

with κ -dependent right-hand side.

To be able to achieve κ -explicit analysis, regularity estimates of the Helmholtz equation are necessary. For convex, or smooth and star-shaped domains, the adjoint Helmholtz problem in Definition 2 satisfies the regularity

$$\|\nabla w\|_{L^2(\Omega)} + \kappa\|w\|_{L^2(\Omega)} + \kappa\|\phi\|_{L^2(\Omega)} \leq C\kappa\|f\|_{L^2(\Omega)}, \quad (4)$$

$$\|\nabla^2 w\|_{L^2(\Omega)} + \kappa\|\nabla \phi\|_{L^2(\Omega)} \leq C(1 + \kappa)\kappa\|f\|_{L^2(\Omega)}, \quad (5)$$

with a constant $C > 0$ independent of κ , see [MPS13, Remark 2.6]. Throughout this study, the H^2 regularity of both BVPs is assumed.

The domain is split into disjoint finite elements T . The set of all finite elements is called \mathcal{T} and there holds $\cup_{T \in \mathcal{T}} T = \Omega$. The facets between elements inside of Ω are denoted by F_I and the facets on $\partial\Omega$ by F_O . If a distinction between

F_I and F_O is not necessary, then a facet will be called F and the set of all facets is defined as \mathcal{F} . The following short notations for L^2 integrals on volume and facet terms are used,

$$(u, v)_T := \int_T u \cdot \bar{v} d\mathbf{x}, \quad (u, v)_F := \int_F u \cdot \bar{v} ds, \quad (6)$$

and the accordingly induced norms are

$$\|u\|_T := \sqrt{(u, u)_T}, \quad \|u\|_F := \sqrt{(u, u)_F}. \quad (7)$$

It is noteworthy that the second argument is complex conjugated. The used discontinuous, complex-valued spaces are defined by:

$$H(\operatorname{div}, T) := \{\sigma \in [L^2(T)]^d : \operatorname{div} \sigma \in L^2(T)\}, \quad (8)$$

$$H(\operatorname{div}, \mathcal{T}) := \prod_{T \in \mathcal{T}} H(\operatorname{div}, T), \quad (9)$$

$$L^2(\mathcal{F}) := \prod_{F \in \mathcal{F}} L^2(F). \quad (10)$$

The respective discrete spaces, of the polynomial degree $p \in \mathbb{N}_0$, are

$$\mathcal{RT}^p(T) := \{\sigma + \mathbf{x} q : \sigma \in [\mathcal{P}^p(T)]^d, q \in \mathcal{P}^p(T)\} \subset H(\operatorname{div}, T), \quad (11)$$

$$\mathcal{RT}^p(\mathcal{T}) := \prod_{T \in \mathcal{T}} \mathcal{RT}^p(T) \subset H(\operatorname{div}, \mathcal{T}), \quad (12)$$

$$\mathcal{P}^p(\mathcal{F}) := \prod_{F \in \mathcal{F}} \mathcal{P}^p(F) \subset L^2(\mathcal{F}), \quad (13)$$

$$\mathcal{P}^p(\mathcal{T}) := \prod_{T \in \mathcal{T}} \mathcal{P}^p(T) \subset L^2(\Omega), \quad (14)$$

where $\mathbf{x} := (x, y, z)^\top$ and \mathcal{P}^p is the space of polynomials with degrees smaller or equal to p . For the discrete, discontinuous compound space the short notation

$$\mathcal{X}_h := \mathcal{RT}^p(\mathcal{T}) \times \mathcal{P}^p(\mathcal{T}) \times \mathcal{P}^p(\mathcal{F}) \times \mathcal{P}^p(\mathcal{F}) \quad (15)$$

is used. The discrete space \mathcal{RT} is commonly known as the Raviart-Thomas space, see [SZ05].

The consistent HDG formulation introduced in [MSS10] and considered in this work is defined as follows.

Definition 4 (HDG Formulation). For given $g \in L^2(\partial\Omega)$ and $\kappa > 0$ find $\sigma \in H(\operatorname{div}, \mathcal{T})$, $u \in L^2(\Omega)$, $\hat{u} \in L^2(\mathcal{F})$, $\hat{\sigma}_{\mathbf{n}} \in L^2(\mathcal{F})$ such that

$$B(\sigma, \hat{\sigma}_{\mathbf{n}}, u, \hat{u}, \tau, \hat{\tau}_{\mathbf{n}}, v, \hat{v}) = -(g, \hat{v})_{\partial\Omega} \quad (16)$$

holds for all $\tau \in H(\operatorname{div}, \mathcal{T})$, $v \in L^2(\Omega)$, $\hat{v} \in L^2(\mathcal{F})$, $\hat{\tau}_{\mathbf{n}} \in L^2(\mathcal{F})$ with the sesquilinear form (SLF)

$$\begin{aligned} B(\sigma, \hat{\sigma}_{\mathbf{n}}, u, \hat{u}, \tau, \hat{\tau}_{\mathbf{n}}, v, \hat{v}) := & \sum_{T \in \mathcal{T}} \left(j\kappa(\sigma, \tau)_T + (u, \operatorname{div} \tau)_T + (\operatorname{div} \sigma, v)_T - j\kappa(u, v)_T \right. \\ & \left. - (\hat{u}, \tau \cdot \mathbf{n})_{\partial T} - (\sigma \cdot \mathbf{n}, \hat{v})_{\partial T} - \alpha([u], [v])_{\partial T} + \beta(\llbracket \sigma \rrbracket, \llbracket \tau \rrbracket)_{\partial T} \right) - (\hat{u}, \hat{v})_{\partial\Omega}. \end{aligned} \quad (17)$$

The jumps are defined as

$$[u] := u - \hat{u}, \quad \llbracket \sigma \rrbracket := \sigma \cdot \mathbf{n} - \hat{\sigma}_{\mathbf{n}}, \quad \text{on } \partial T \quad (18)$$

and the stabilisation parameters are $\alpha := 1$, $\beta := 1$.

The normal vector \mathbf{n} is per default outward-oriented on T and the use as the subscript for the facet variables $\hat{\sigma}_{\mathbf{n}}$ and $\hat{\tau}_{\mathbf{n}}$ indicates that the variables are scalar-valued and their sign changes with respect to the adjacent elements.

Remark 5. An interesting property of the HDG formulation is the choice of the h -independent parameters α and β . The reason for the choices in this study is due to the favourable properties for iterative solvers and their preconditioning established in [Hub13, HPS13, HS14].

For methods with static condensation, the sub-problems defined on individual elements must be uniquely and stably solvable. The HDG formulation (16) satisfies that condition and the following discrete absolute stability result holds.

Theorem 6. *Assuming H^2 -regularity of the adjoint problem, there exists a constant $\tilde{C} > 0$, independent of κ, h, α, β , so that there holds for the discrete solution of the HDG formulation (16)*

$$\sum_{T \in \mathcal{T}} \alpha \| [u_h] \|_{L^2(\partial T)}^2 + \beta \| [\sigma_h] \|_{L^2(\partial T)}^2 + \| \hat{u}_h \|_{L^2(\partial \Omega)}^2 \leq \| g \|_{L^2(\partial \Omega)}^2, \quad (19)$$

$$\sum_{T \in \mathcal{T}} \kappa \| \sigma_h \|_{L^2(T)}^2 \leq \sum_{T \in \mathcal{T}} \kappa \| u_h \|_{L^2(T)}^2 + \| g \|_{L^2(\partial \Omega)}^2, \quad (20)$$

$$\| u_h \|_{L^2(\Omega)} \leq C(\kappa, h, \alpha, \beta) \| g \|_{L^2(\partial \Omega)}, \quad (21)$$

with the constant

$$C(\kappa, h, \alpha, \beta) = \tilde{C} \left(\left(\frac{2}{\alpha} + \beta \right) (1 + \kappa)^2 h + 2\alpha(1 + \kappa)^2 \kappa^2 h^3 + 1 \right)^{\frac{1}{2}}. \quad (22)$$

This theorem implies the existence and uniqueness of the discrete solution for the HDG formulation, without a resolution condition on the discrete space. The proof uses a similar approach as introduced in [LCQ17] for Maxwell's equations. Two major differences are that only a single facet space is used in the mentioned work and the stabilisation parameter therein is h -dependent. The method in [LCQ17] is related to the case of choosing $\alpha \approx \frac{1}{h}$, $\beta = 0$ and omitting the second facet variable in the HDG formulation (16). The main idea of the proof is to use an Aubin-Nitsche technique along with L^2 -projections of σ and u so that volume terms vanish and only facet terms remain. The real part of the HDG formulation controls those facet terms. With similar techniques and arguments, the following optimal convergence rates for jumps and the pressure are proven.

Theorem 7. *Assuming H^{p+2} -regularity of the Helmholtz problem, there exists a constant $C > 0$, independent of κ, h, α, β , such that*

$$\begin{aligned} \sum_{T \in \mathcal{T}} \alpha \| [u - u_h] \|_{L^2(\partial T)}^2 + \beta \| [\sigma - \sigma_h] \|_{L^2(\partial T)}^2 + \| u - \hat{u}_h \|_{L^2(\partial \Omega)}^2 \\ \leq C h^{2p+1} \left(\left(\frac{2}{\alpha} + \beta \right) \| \sigma \|_{H^{p+1}(\Omega)}^2 + 2\alpha \| u \|_{H^{p+1}(\Omega)}^2 \right). \end{aligned} \quad (23)$$

Theorem 8. *Assuming H^2 -regularity of the adjoint problem and H^{p+2} -regularity of the Helmholtz problem, there exists a constant $C > 0$, independent of κ, h, α, β , such that*

$$\begin{aligned} \| u - u_h \|_{L^2(\Omega)} \\ \leq C h^{p+1} \left(\left(\frac{2}{\alpha} + \beta \right) (1 + \kappa)^2 + 2\alpha(1 + \kappa)^2 \kappa^2 h^2 \right)^{\frac{1}{2}} \left(\left(\frac{2}{\alpha} + \beta \right) \| \sigma \|_{H^{p+1}(\Omega)}^2 + 2\alpha \| u \|_{H^{p+1}(\Omega)}^2 \right)^{\frac{1}{2}}. \end{aligned} \quad (24)$$

Due to the h -independent stabilisation, the optimal convergence rate for the flux cannot be straightforwardly derived. For the following result, a more refined technique based on projections is needed.

Theorem 9. *Assuming H^2 -regularity of the adjoint problem and H^{p+2} -regularity of the Helmholtz problem, there exists a constant $C(\kappa, \alpha, \beta) > 0$, independent of h , such that*

$$\| \sigma - \sigma_h \|_{L^2(\Omega)} \leq C(\kappa, \alpha, \beta) h^{p+1} (\| \sigma \|_{H^{p+1}(\Omega)} + \| u \|_{H^{p+1}(\Omega)}). \quad (25)$$

The explicit form of $C(\kappa, \alpha, \beta)$ can be seen in Section 5. The contribution of [GM11], which is based upon the techniques developed in [CGS10], motivates the proof of this theorem. A comprehensive and thorough explanation of the later work can be found in [Say13]. In these studies, HDG methods with h -independent stabilisation are analysed. The HDG formulation in [GM11] is similar to the formulation in this work. The first major difference is that only a single facet variable with a comparable α -stabilisation is used and the second is that existence, uniqueness and optimal convergence rates are proven under the assumption of a resolution condition. Proving optimal rates for h -independently stabilised HDG formulation is challenging, because element boundary terms need to be estimated via an inverse estimate with volume terms leading to sub-optimal rates. The idea is to use a, to the HDG formulation tailored, projection into the discrete space, so that boundary terms vanish. For that purpose, a special projection has been established and analysed in [CGS10]. In this study, due to the second β -stabilisation, that projection cannot be applied. A generalisation needs to be established for the proof.

3 Discrete Absolute Stability

Usually, for finite element discretisations of the Helmholtz equation, a resolution condition is required to prove the existence and uniqueness of discrete solutions as well as quasi-optimality. These results hold in the asymptotic regime. Several publications have established the existence and uniqueness for DG and HDG methods without such a condition, e.g. [FW09, FW11, FX13, MPS13, MS14, Wu14, FLX16]. The idea is to use the discrete test function $\mathbf{x} \cdot \nabla u_h$ which is contained in the discrete discontinuous space and leads to positive volume terms. The disadvantage is that the pre-asymptotic and the asymptotic analysis require different techniques.

A new approach based upon L^2 -projections, which leads to results viable in the pre-asymptotic as well as the asymptotic regime, has been developed in [LCQ17]. In this section, the technique therein is applied to the HDG formulation (16), with the additional consideration of a second facet variable and β -stabilisation as well as h -independent α -stabilisation.

The following lemma establishes the consistency of the adjoint Helmholtz problem in Definition 2.

Lemma 10 (Weak Adjoint Formulation). *The adjoint solution (ϕ, w) of (2a) - (2c), satisfies*

$$B(\tau_h, \hat{\tau}_{\mathbf{n},h}, v_h, \hat{v}_h, \phi, \phi \cdot \mathbf{n}, w, w) = (v_h, f)_\Omega, \quad (26)$$

for all $(\tau_h, \hat{\tau}_{\mathbf{n},h}, v_h, \hat{v}_h) \in \mathcal{X}_h$.

Proof. Conjugating (2a) and (2b) leads to

$$-j\kappa\bar{\phi} + \nabla\bar{w} = 0, \quad (27)$$

$$-\operatorname{div}\bar{\phi} + j\kappa\bar{w} = -\bar{f}, \quad (28)$$

further multiplying by τ_h, v_h respectively and integrating over T gives

$$-j\kappa(\tau_h, \phi)_T + (\tau_h, \nabla w)_T = 0, \quad (29)$$

$$-(v_h, \operatorname{div}\phi)_T + j\kappa(v_h, w)_T = -(v_h, f)_T. \quad (30)$$

Element wise partial integration of $(\tau_h, \nabla w)_T$ and summation over all elements results in

$$\sum_{T \in \mathcal{T}} j\kappa(\tau_h, \phi)_T + (\operatorname{div}\tau_h, w)_T + (v_h, \operatorname{div}\phi)_T - j\kappa(v_h, w)_T - (\tau_h \cdot \mathbf{n}, w)_{\partial T} = (v_h, f)_\Omega. \quad (31)$$

Whenever jumps between variables on adjacent elements over facets are considered, then one side is marked by the $+$ -subscript and the other by $-$. The normal continuity of ϕ on F_1 implies

$$0 = -(\hat{v}_h, \phi_+ \cdot \mathbf{n}_+ - \phi_- \cdot \mathbf{n}_+)_{F_1} = -(\hat{v}_h, \phi_+ \cdot \mathbf{n}_+)_{F_1} - (\hat{v}_h, \phi_- \cdot \mathbf{n}_-)_{F_1} \quad (32)$$

and due to the boundary condition (2c) there holds

$$0 = -(\hat{v}_h, \phi \cdot \mathbf{n})_{\partial\Omega} - (\hat{v}_h, w)_{\partial\Omega}. \quad (33)$$

Adding these terms and considering that the α - and β -stabilisations vanish due to the continuity of $\phi \cdot \mathbf{n}$ and w on element boundaries concludes the proof. \square

The following first stability results follow by considering the real (\Re) and imaginary (\Im) part of the SLF B separately. This lemma and the proof of it are similar to [LCQ17, Lemma 3.1].

Lemma 11. *For the discrete solution of (16) there holds*

$$\sum_{T \in \mathcal{T}} \alpha \| [u_h] \|_{\partial T}^2 + \beta \| \llbracket \sigma_h \rrbracket \|_{\partial T}^2 + \| \hat{u}_h \|_{\partial\Omega}^2 \leq \| g \|_{\partial\Omega}^2, \quad (34)$$

$$\sum_{T \in \mathcal{T}} \kappa \| \sigma_h \|_T^2 \leq \sum_{T \in \mathcal{T}} \kappa \| u_h \|_T^2 + \| g \|_{\partial\Omega}^2. \quad (35)$$

Proof. By choosing $v_h = -u_h, \tau_h = \sigma_h, \hat{v}_h = -\hat{u}_h, \hat{\tau}_{\mathbf{n},h} = \hat{\sigma}_{\mathbf{n},h}$ as test functions B has the form

$$\begin{aligned} B(\sigma_h, \hat{\sigma}_{\mathbf{n},h}, u_h, \hat{u}_h, \sigma_h, \hat{\sigma}_{\mathbf{n},h}, -u_h, -\hat{u}_h) &= \sum_{T \in \mathcal{T}} j\kappa \| \sigma_h \|_T^2 + 2\Im(u_h, \operatorname{div}\sigma_h)_T + j\kappa \| u_h \|_T^2 \\ &\quad - 2\Im(\hat{u}_h, \sigma_h \cdot \mathbf{n})_{\partial T} + \alpha \| [u_h] \|_{\partial T}^2 + \beta \| \llbracket \sigma_h \rrbracket \|_{\partial T}^2 + \| \hat{u}_h \|_{\partial\Omega}^2. \end{aligned} \quad (36)$$

Taking the real part leads to

$$\alpha\| [u_h] \|_{\partial T}^2 + \beta\| [\sigma_h] \|_{\partial T}^2 + \|\hat{u}_h\|_{\partial\Omega}^2 = \Re(g, \hat{u}_h)_{\partial\Omega} \quad (37)$$

directly implying (34). Similarly, choosing $v_h = u_h, \tau_h = \sigma_h, \hat{v}_h = \hat{u}_h, \hat{\tau}_{n,h} = \hat{\sigma}_{n,h}$ as test functions gives

$$\begin{aligned} B(\sigma_h, \hat{\sigma}_{n,h}, u_h, \hat{u}_h, \sigma_h, \hat{\sigma}_{n,h}, u_h, \hat{u}_h) &= \sum_{T \in \mathcal{T}} j\kappa \|\sigma_h\|_T^2 + 2\Re(u_h, \operatorname{div} \sigma_h)_T - j\kappa \|u_h\|_T^2 \\ &\quad - 2\Re(\hat{u}_h, \sigma_h \cdot \mathbf{n})_{\partial T} - \alpha\| [u_h] \|_{\partial T}^2 + \beta\| [\sigma_h] \|_{\partial T}^2 - \|\hat{u}_h\|_{\partial\Omega}^2. \end{aligned} \quad (38)$$

Taking the imaginary part yields

$$\sum_{T \in \mathcal{T}} \kappa \|\sigma_h\|_T^2 - \kappa \|u_h\|_T^2 = -\Im(g, \hat{u}_h)_{\partial\Omega}, \quad (39)$$

and with (34), which implies $\|\hat{u}_h\|_{\partial\Omega} \leq \|g\|_{\partial\Omega}$, gives (35). \square

Lemma 11 shows that \hat{u}_h and the discrete jumps are bounded by the excitation, and if u_h can be bounded then the same follows for σ_h . The result highlights the favourable choice of real, positive α and β . The adjoint problem in combination with an Aubin-Nitsche type technique is used to bound u_h .

Lemma 12. *For the solution (ϕ, w) of (2a) - (2c) there holds*

$$\|w\|_{\partial\Omega}^2 = \|\phi \cdot \mathbf{n}\|_{\partial\Omega}^2 \leq C\|f\|_{\Omega}^2, \quad (40)$$

with a constant $C > 0$ independent of κ .

Proof. The first equality immediately follows from (2c). Multiplying (2a) and (2b) by $\bar{\phi}$ and \bar{w} respectively gives

$$j\kappa\|\phi\|_{\Omega}^2 + (\nabla w, \phi)_{\Omega} = 0, \quad (41)$$

$$j\kappa\|w\|_{\Omega}^2 + (\operatorname{div} \phi, w)_{\Omega} = (f, w)_{\Omega}. \quad (42)$$

Partial integration of $(\nabla w, \phi)_{\Omega}$ leads to

$$j\kappa\|\phi\|_{\Omega}^2 - (w, \operatorname{div} \phi)_{\Omega} + (w, \phi \cdot \mathbf{n})_{\partial\Omega} = 0. \quad (43)$$

By conjugating and adding the equations the terms $(\operatorname{div} \phi, w)_{\Omega}$ cancel out and

$$j\kappa\|w\|_{\Omega}^2 - j\kappa\|\phi\|_{\Omega}^2 + (\phi \cdot \mathbf{n}, w)_{\partial\Omega} = (f, w)_{\Omega} \quad (44)$$

remains. Using (2c) and only considering the real part in combination with the adjoint regularity implies

$$\|\phi \cdot \mathbf{n}\|_{\partial\Omega}^2 \leq \frac{1}{\kappa}\|f\|_{\Omega}\kappa\|w\|_{\Omega} \leq C\|f\|_{\Omega}^2. \quad (45)$$

\square

The following lemma is essential for pre-asymptotic stability. It highlights the effect of introducing L^2 -projections of σ and u defined by

$$(\Pi\sigma, \tau_h)_T = (\sigma, \tau_h)_T \quad \forall \tau_h \in \mathcal{RT}^p(T), \quad (46)$$

$$(\Pi u, v_h)_T = (u, v_h)_T \quad \forall v_h \in \mathcal{P}^p(T), \quad (47)$$

$$(\Pi_F u, \hat{v}_h)_F = (u, \hat{v}_h)_F \quad \forall \hat{v}_h \in \mathcal{P}^p(F), \quad (48)$$

into the SLF. The proof follows the lines in [LCQ17, Lemma 3.2].

Lemma 13. *Using the L^2 -projection Π on elements and the L^2 -projection Π_F on facets, there holds for arbitrary $\tau_h, \hat{\tau}_{n,h}, v_h, \hat{v}_h \in \mathcal{X}_h$*

$$\begin{aligned} B(\tau_h, \hat{\tau}_{n,h}, v_h, \hat{v}_h, \phi - \Pi\phi, \phi \cdot \mathbf{n} - \Pi_F\phi \cdot \mathbf{n}, w - \Pi w, w - \Pi_F w) \\ = \sum_{T \in \mathcal{T}} ([v_h], (\phi - \Pi\phi) \cdot \mathbf{n})_{\partial T} - \alpha([v_h], w - \Pi w)_{\partial T} + \beta([\tau_h], (\phi - \Pi\phi) \cdot \mathbf{n})_{\partial T}. \end{aligned} \quad (49)$$

Proof. The expression on the left-hand side of the equation is

$$\begin{aligned}
 & B(\tau_h, \hat{\tau}_{\mathbf{n},h}, v_h, \hat{v}_h, \phi - \Pi\phi, \phi \cdot \mathbf{n} - \Pi_F\phi \cdot \mathbf{n}, w - \Pi w, w - \Pi_F w) \\
 &= \sum_{T \in \mathcal{T}} j\kappa(\tau_h, \phi - \Pi\phi)_T + (v_h, \operatorname{div}(\phi - \Pi\phi))_T + (\operatorname{div} \tau_h, w - \Pi w)_T - j\kappa(v_h, w - \Pi w)_T \\
 &\quad - (\hat{v}_h, (\phi - \Pi\phi) \cdot \mathbf{n})_{\partial T} - (\tau_h \cdot \mathbf{n}, w - \Pi_F w)_{\partial T} \\
 &\quad - \alpha([v_h], [w - \Pi w])_{\partial T} + \beta(\llbracket \tau_h \rrbracket, \llbracket \phi - \Pi\phi \rrbracket)_{\partial T} - (\hat{v}_h, w - \Pi_F w)_{\partial \Omega}.
 \end{aligned} \tag{50}$$

Due to the L^2 -projection properties the terms

$$j\kappa(\tau_h, \phi - \Pi\phi)_T = 0, \quad (\operatorname{div} \tau_h, w - \Pi w)_T = 0, \quad -j\kappa(v_h, w - \Pi w)_T = 0, \tag{51}$$

$$-(\tau_h \cdot \mathbf{n}, w - \Pi_F w)_{\partial T} = 0, \quad -(\hat{v}_h, w - \Pi_F w)_{\partial \Omega} = 0 \tag{52}$$

vanish. The remaining volume term introduces, after partial integration, the following element boundary terms

$$(v_h, \operatorname{div}(\phi - \Pi\phi))_T = -(\nabla v_h, \phi - \Pi\phi)_T + (v_h, (\phi - \Pi\phi) \cdot \mathbf{n})_{\partial T} = (v_h, (\phi - \Pi\phi) \cdot \mathbf{n})_{\partial T} \tag{53}$$

and for jumps there hold

$$-\alpha([v_h], [w - \Pi w])_{\partial T} = -\alpha([v_h], w - \Pi w - w + \Pi_F w)_{\partial T} = -\alpha([v_h], w - \Pi w)_{\partial T}, \tag{54}$$

$$\beta(\llbracket \tau_h \rrbracket, \llbracket \phi - \Pi\phi \rrbracket)_{\partial T} = \beta(\llbracket \tau_h \rrbracket, (\phi - \Pi\phi) \cdot \mathbf{n})_{\partial T}. \tag{55}$$

Incorporating these changes yields

$$\begin{aligned}
 & B(\tau_h, \hat{\tau}_{\mathbf{n},h}, v_h, \hat{v}_h, \phi - \Pi\phi, \phi_{\mathbf{n}} - \Pi_F\phi_{\mathbf{n}}, w - \Pi w, w - \Pi_F w) \\
 &= \sum_{T \in \mathcal{T}} (v_h - \hat{v}_h, (\phi - \Pi\phi) \cdot \mathbf{n})_{\partial T} - \alpha([v_h], w - \Pi w)_{\partial T} + \beta(\llbracket \tau_h \rrbracket, (\phi - \Pi\phi) \cdot \mathbf{n})_{\partial T}.
 \end{aligned} \tag{56}$$

□

To prove the main result of this section the following standard approximation properties of L^2 -projections are required.

Lemma 14 (Approximation Properties of L^2 -projections). *Assuming H^{s+1} -regularity of ϕ , H^{t+1} -regularity of w , with $s, t \in \mathbb{R}_+$. If the polynomial degree of the discrete spaces satisfies $p \geq s \geq 0$, $p \geq t \geq 0$, then exists a constant $C > 0$ independent of h so that*

$$\sum_{T \in \mathcal{T}} \|(\phi - \Pi\phi) \cdot \mathbf{n}\|_{\partial T}^2 \leq Ch^{2s+1} \|\phi\|_{H^{s+1}}^2, \tag{57}$$

$$\sum_{T \in \mathcal{T}} \|w - \Pi w\|_{\partial T}^2 \leq Ch^{2t+1} \|w\|_{H^{t+1}}^2. \tag{58}$$

In the following theorem u_h will be bounded by g , which concludes the stability analysis of the HDG formulation. The proof is based upon [LCQ17, Lemma 3.2].

Proof of Theorem 6. Using an Aubin-Nitsche trick for the adjoint problem, by considering as excitation $f = u_h$, yields in combination with Lemma 10

$$\|u_h\|_{\Omega}^2 = B(\sigma_h, \hat{\sigma}_{\mathbf{n},h}, u_h, \hat{u}_h, \phi, \phi_{\mathbf{n}}, w, w), \tag{59}$$

with $(\sigma_h, \hat{\sigma}_{\mathbf{n},h}, u_h, \hat{u}_h)$ as test functions. Adding and subtracting the L^2 -projections Π and Π_F leads to

$$\begin{aligned}
 \|u_h\|_{\Omega}^2 &= B(\sigma_h, \hat{\sigma}_{\mathbf{n},h}, u_h, \hat{u}_h, \phi - \Pi\phi, \phi_{\mathbf{n}} - \Pi_F\phi_{\mathbf{n}}, w - \Pi w, w - \Pi_F w) \\
 &\quad + B(\sigma_h, \hat{\sigma}_{\mathbf{n},h}, u_h, \hat{u}_h, \Pi\phi, \Pi_F\phi_{\mathbf{n}}, \Pi w, \Pi_F w).
 \end{aligned} \tag{60}$$

The first part is replaced by Lemma 13 and according to (16) there holds for the second part

$$B(\sigma_h, \hat{\sigma}_{\mathbf{n},h}, u_h, \hat{u}_h, \Pi\phi, \Pi_F\phi_{\mathbf{n}}, \Pi w, \Pi_F w) = -(g, \Pi_F w)_{\partial \Omega}, \tag{61}$$

because the projected adjoint solution is in the discrete space \mathcal{X}_h . Cauchy-Schwarz and Lemma 11 give the estimate

$$\begin{aligned}
 \|u_h\|_{\Omega}^2 &= \sum_{T \in \mathcal{T}} ([u_h], (\phi - \Pi\phi) \cdot \mathbf{n})_{\partial T} - \alpha([u_h], w - \Pi w)_{\partial T} + \beta([\sigma_h], (\phi - \Pi\phi) \cdot \mathbf{n})_{\partial T} - (g, \Pi_F w)_{\partial\Omega} \\
 &\leq \left(\sum_{T \in \mathcal{T}} \alpha \| [u_h] \|_{\partial T}^2 + \beta \| [\sigma_h] \|_{\partial T}^2 + \|g\|_{\partial\Omega}^2 \right)^{\frac{1}{2}} \\
 &\quad \left(\sum_{T \in \mathcal{T}} \frac{2}{\alpha} \| (\phi - \Pi\phi) \cdot \mathbf{n} \|_{\partial T}^2 + 2\alpha \|w - \Pi w\|_{\partial T}^2 + \beta \| (\phi - \Pi\phi) \cdot \mathbf{n} \|_{\partial T}^2 + \| \Pi_F w \|_{\partial\Omega}^2 \right)^{\frac{1}{2}} \\
 &\leq \sqrt{2} \|g\|_{\partial\Omega} \left(\sum_{T \in \mathcal{T}} \frac{2}{\alpha} \| (\phi - \Pi\phi) \cdot \mathbf{n} \|_{\partial T}^2 + 2\alpha \|w - \Pi w\|_{\partial T}^2 + \beta \| (\phi - \Pi\phi) \cdot \mathbf{n} \|_{\partial T}^2 + \| \Pi_F w \|_{\partial\Omega}^2 \right)^{\frac{1}{2}},
 \end{aligned} \tag{62}$$

and further applying the L^2 approximation properties and Lemma 12 for the term on the domain boundary yields

$$\|u_h\|_{\Omega}^2 \leq C \|g\|_{\partial\Omega} \left(\left(\frac{2}{\alpha} + \beta \right) h^{2s+1} \|\phi\|_{H^{s+1}}^2 + 2\alpha h^{2t+1} \|w\|_{H^{t+1}}^2 + \|u_h\|_{\Omega}^2 \right)^{\frac{1}{2}}. \tag{63}$$

Due to the H^2 -regularity of the adjoint problem $s = 0, t = 1$ can be chosen leading to the stability constant

$$C(\kappa, h, \alpha, \beta) = C \left(\left(\frac{2}{\alpha} + \beta \right) (1 + \kappa)^2 h + 2\alpha(1 + \kappa)^2 \kappa^2 h^3 + 1 \right)^{\frac{1}{2}}. \tag{64}$$

□

4 Error Estimates for the Pressure and Jumps

In this section Theorem 7 and Theorem 8 are proven. The analysis is similar to the proof of stability in the last section and leans on [LCQ17]. The continuous and discrete solutions satisfy

$$\begin{aligned}
 B(\sigma, \sigma_{\mathbf{n}}, u, u, \tau_h, \hat{\tau}_{\mathbf{n},h}, v_h, \hat{v}_h) &= -(g, \hat{v}_h)_{\partial\Omega}, \\
 B(\sigma_h, \hat{\sigma}_{\mathbf{n},h}, u_h, \hat{u}_h, \tau_h, \hat{\tau}_{\mathbf{n},h}, v_h, \hat{v}_h) &= -(g, \hat{v}_h)_{\partial\Omega},
 \end{aligned} \tag{65}$$

for all $(\tau_h, \hat{\tau}_{\mathbf{n},h}, v_h, \hat{v}_h) \in \mathcal{X}_h$. In the case of coercive weak formulations optimal convergence rates are proven with coercivity, Galerkin orthogonality and continuity. The Helmholtz equation does not satisfy coercivity, therefore other techniques need to be established. Usually, a Schatz argument is applied to derive asymptotic results, but these depend on a resolution condition. The L^2 -projections circumvent this necessity.

For the analysis, the following projected errors, contained in the discontinuous space \mathcal{X}_h , are needed.

Definition 15.

$$e_{\sigma} := \Pi\sigma - \sigma_h, \quad e_u := \Pi u - u_h, \quad e_{\hat{u}} := \Pi_F u - \hat{u}_h, \quad e_{\hat{\sigma}} := \Pi_F \sigma \cdot \mathbf{n} - \hat{\sigma}_{\mathbf{n},h}. \tag{66}$$

Projections lead to a splitting of error estimates into e.g.

$$\|u - u_h\|_{\Omega} = \|u - \Pi u + \Pi u - u_h\|_{\Omega} \leq \|u - \Pi u\|_{\Omega} + \|\Pi u - u_h\|_{\Omega}. \tag{67}$$

The first part only depends on the approximation properties of the projection. The second part holds the advantage that $\Pi u - u_h$ is a viable choice as a discrete test function. Therefore, if the projection has optimal approximation properties and if the projected error has an optimal convergence rate, then the discrete solution has an optimal rate as well.

For the projected errors the Galerkin orthogonality does not hold, but they satisfy the following discrete weak formulation.

Lemma 16. *The projected errors in (66) satisfy the weak formulation*

$$\begin{aligned}
 B(e_{\sigma}, e_{\hat{\sigma}}, e_u, e_{\hat{u}}, \tau_h, \hat{\tau}_{\mathbf{n},h}, v_h, \hat{v}_h) \\
 = - \sum_{T \in \mathcal{T}} (\sigma \cdot \mathbf{n} - \Pi\sigma \cdot \mathbf{n}, [v_h])_{\partial T} - \alpha(u - \Pi u, [v_h])_{\partial T} + \beta(\sigma \cdot \mathbf{n} - \Pi\sigma \cdot \mathbf{n}, [\tau_h])_{\partial T},
 \end{aligned} \tag{68}$$

for all $(\tau_h, \hat{\tau}_{\mathbf{n},h}, v_h, \hat{v}_h) \in \mathcal{X}_h$.

Proof. By testing with discrete functions, continuous variables can be replaced with their Π_F -projections on facets. The volume projection Π can be inserted into most parts, except for

$$\begin{aligned} \sum_{T \in \mathcal{T}} (\operatorname{div} \sigma, v_h)_T &= \sum_{T \in \mathcal{T}} -(\sigma, \nabla v_h)_T + (\Pi_F \sigma \cdot \mathbf{n}, v_h)_{\partial T} \\ &= \sum_{T \in \mathcal{T}} -(\Pi \sigma, \nabla v_h)_T + (\Pi_F \sigma \cdot \mathbf{n}, v_h)_{\partial T} \\ &= \sum_{T \in \mathcal{T}} (\operatorname{div} \Pi \sigma, v_h)_T + (\Pi_F \sigma \cdot \mathbf{n} - \Pi \sigma \cdot \mathbf{n}, v_h)_{\partial T}, \end{aligned} \quad (69)$$

which results in boundary terms. Taking them into account yields

$$\begin{aligned} &B(\sigma, \sigma_{\mathbf{n}}, u, u, \tau_h, \hat{\tau}_{\mathbf{n},h}, v_h, \hat{v}_h) \\ &= \sum_{T \in \mathcal{T}} j\kappa(\Pi \sigma, \tau_h)_T + (\Pi u, \operatorname{div} \tau_h)_T + (\operatorname{div} \Pi \sigma, v_h)_T - j\kappa(\Pi u, v_h)_T + (\Pi_F \sigma \cdot \mathbf{n} - \Pi \sigma \cdot \mathbf{n}, v_h)_{\partial T} \\ &\quad - (\Pi_F u, \tau_h \cdot \mathbf{n})_{\partial T} - (\Pi_F \sigma \cdot \mathbf{n}, \hat{v}_h)_{\partial T} - \alpha(\Pi_F[u], [v_h])_{\partial T} + \beta(\Pi_F[\sigma], \llbracket \tau_h \rrbracket)_{\partial T} - (\Pi_F u, \hat{v}_h)_{\partial \Omega}, \end{aligned} \quad (70)$$

which leads to

$$\begin{aligned} 0 &= B(\sigma, \sigma_{\mathbf{n}}, u, u, \tau_h, \hat{\tau}_{\mathbf{n},h}, v_h, \hat{v}_h) - B(\sigma_h, \hat{\sigma}_{\mathbf{n},h}, u_h, \hat{u}_h, \tau_h, \hat{\tau}_{\mathbf{n},h}, v_h, \hat{v}_h) \\ &= \sum_{T \in \mathcal{T}} j\kappa(e_\sigma, \tau_h)_T + (e_u, \operatorname{div} \tau_h)_T + (\operatorname{div} e_\sigma, v_h)_T - j\kappa(e_u, v_h)_T \\ &\quad + (\Pi_F \sigma \cdot \mathbf{n} - \Pi \sigma \cdot \mathbf{n}, v_h)_{\partial T} - (e_{\hat{u}}, \tau_h \cdot \mathbf{n})_{\partial T} - (\Pi_F \sigma \cdot \mathbf{n} - \sigma_h \cdot \mathbf{n}, \hat{v}_h)_{\partial T} \\ &\quad - \alpha(\Pi_F[u] - [u_h], [v_h])_{\partial T} + \beta(\Pi_F[\sigma] - \llbracket \sigma_h \rrbracket, \llbracket \tau_h \rrbracket)_{\partial T} - (e_{\hat{u}}, \hat{v}_h)_{\partial \Omega}. \end{aligned} \quad (71)$$

There hold the following identities on element boundaries:

$$\begin{aligned} \Pi_F \sigma \cdot \mathbf{n} - \sigma_h \cdot \mathbf{n} &= \Pi_F \sigma \cdot \mathbf{n} - \Pi \sigma \cdot \mathbf{n} + \Pi \sigma \cdot \mathbf{n} - \sigma_h \cdot \mathbf{n} \\ &= e_\sigma \cdot \mathbf{n} - (\Pi \sigma \cdot \mathbf{n} - \Pi_F \sigma \cdot \mathbf{n}), \end{aligned} \quad (72)$$

$$\begin{aligned} \Pi_F u - \Pi_F u - u_h + \hat{u}_h &= \Pi u - u_h - \Pi_F u + \hat{u}_h - \Pi u + \Pi_F u \\ &= e_u - e_{\hat{u}} - (\Pi u - \Pi_F u), \end{aligned} \quad (73)$$

$$\begin{aligned} \Pi_F \sigma \cdot \mathbf{n} - \Pi_F \sigma \cdot \mathbf{n} - \sigma_h \cdot \mathbf{n} + \hat{\sigma}_{\mathbf{n},h} &= \Pi \sigma \cdot \mathbf{n} - \sigma_h \cdot \mathbf{n} - \Pi_F \sigma \cdot \mathbf{n} + \hat{\sigma}_{\mathbf{n},h} - (\Pi \sigma \cdot \mathbf{n} - \Pi_F \sigma \cdot \mathbf{n}) \\ &= e_\sigma \cdot \mathbf{n} - e_{\hat{\sigma}} - (\Pi \sigma \cdot \mathbf{n} - \Pi_F \sigma \cdot \mathbf{n}). \end{aligned} \quad (74)$$

Replacing the appropriate terms results in

$$\begin{aligned} 0 &= \sum_{T \in \mathcal{T}} j\kappa(e_\sigma, \tau_h)_T + (e_u, \operatorname{div} \tau_h)_T + (\operatorname{div} e_\sigma, v_h)_T - j\kappa(e_u, v_h)_T \\ &\quad + (\Pi_F \sigma \cdot \mathbf{n} - \Pi \sigma \cdot \mathbf{n}, v_h)_{\partial T} - (e_{\hat{u}}, \tau_h \cdot \mathbf{n})_{\partial T} - (e_\sigma \cdot \mathbf{n} - (\Pi \sigma \cdot \mathbf{n} - \Pi_F \sigma \cdot \mathbf{n}), \hat{v}_h)_{\partial T} \\ &\quad - \alpha(e_u - e_{\hat{u}} - (\Pi u - \Pi_F u), [v_h])_{\partial T} + \beta(e_\sigma \cdot \mathbf{n} - e_{\hat{\sigma}} - (\Pi \sigma \cdot \mathbf{n} - \Pi_F \sigma \cdot \mathbf{n}), \llbracket \tau_h \rrbracket)_{\partial T} - (e_{\hat{u}}, \hat{v}_h)_{\partial \Omega} \\ &= B(e_\sigma, e_{\hat{\sigma}}, e_u, e_{\hat{u}}, \tau_h, \hat{\tau}_{\mathbf{n},h}, v_h, \hat{v}_h) \\ &\quad + \sum_{T \in \mathcal{T}} -(\Pi \sigma \cdot \mathbf{n} - \Pi_F \sigma \cdot \mathbf{n}, [v_h])_{\partial T} + \alpha(\Pi u - \Pi_F u, [v_h])_{\partial T} - \beta(\Pi \sigma \cdot \mathbf{n} - \Pi_F \sigma \cdot \mathbf{n}, \llbracket \tau_h \rrbracket)_{\partial T}, \end{aligned} \quad (75)$$

which concludes the proof. \square

With the previous lemma Theorem 7 can be shown.

Proof of Theorem 7. The proof is similar to [LCQ17, Lemma 4.2]. Setting $\tau_h := e_\sigma$, $\hat{\tau}_{\mathbf{n},h} := e_{\hat{\sigma}}$, $v_h := -e_u$, $\hat{v}_h := -e_{\hat{u}}$ in Lemma 16 yields

$$\begin{aligned} &B(e_\sigma, e_{\hat{\sigma}}, e_u, e_{\hat{u}}, e_\sigma, e_{\hat{\sigma}}, -e_u, -e_{\hat{u}}) \\ &= \sum_{T \in \mathcal{T}} j\kappa \|e_\sigma\|_T^2 + 2\Im(e_u, \operatorname{div} e_\sigma)_T + j\kappa \|e_u\|_T^2 - 2\Im(e_{\hat{u}}, e_\sigma \cdot \mathbf{n})_{\partial T} + \alpha \|[e_u]\|_{\partial T}^2 + \beta \|\llbracket e_\sigma \rrbracket\|_{\partial T}^2 + \|e_{\hat{u}}\|_{\partial \Omega}^2 \\ &= \sum_{T \in \mathcal{T}} -(\Pi \sigma \cdot \mathbf{n} - \sigma \cdot \mathbf{n}, [e_u])_{\partial T} + \alpha(\Pi u - u, [e_u])_{\partial T} + \beta(\Pi \sigma \cdot \mathbf{n} - \sigma \cdot \mathbf{n}, \llbracket e_\sigma \rrbracket)_{\partial T} \end{aligned} \quad (76)$$

and considering the real part gives

$$\begin{aligned} & \sum_{T \in \mathcal{T}} \alpha \| [e_u] \|_{\partial T}^2 + \beta \| \llbracket e_\sigma \rrbracket \|_{\partial T}^2 + \| e_{\hat{u}} \|_{\partial \Omega}^2 \\ &= \Re \sum_{T \in \mathcal{T}} -(\Pi \sigma \cdot \mathbf{n} - \sigma \cdot \mathbf{n}, [e_u])_{\partial T} + \alpha (\Pi u - u, [e_u])_{\partial T} + \beta (\Pi \sigma \cdot \mathbf{n} - \sigma \cdot \mathbf{n}, \llbracket e_\sigma \rrbracket)_{\partial T}. \end{aligned} \quad (77)$$

The right-hand side can be estimated by

$$\begin{aligned} & \left| \sum_{T \in \mathcal{T}} -(\Pi \sigma \cdot \mathbf{n} - \sigma \cdot \mathbf{n}, [e_u])_{\partial T} + \alpha (\Pi u - u, [e_u])_{\partial T} + \beta (\Pi \sigma \cdot \mathbf{n} - \sigma \cdot \mathbf{n}, \llbracket e_\sigma \rrbracket)_{\partial T} \right| \\ & \leq \left(\sum_{T \in \mathcal{T}} \frac{2}{\alpha} \| \Pi \sigma \cdot \mathbf{n} - \sigma \cdot \mathbf{n} \|_{\partial T}^2 + 2\alpha \| \Pi u - u \|_{\partial T}^2 + \beta \| \Pi \sigma \cdot \mathbf{n} - \sigma \cdot \mathbf{n} \|_{\partial T}^2 \right)^{\frac{1}{2}} \left(\sum_{T \in \mathcal{T}} \alpha \| [e_u] \|_{\partial T}^2 + \beta \| \llbracket e_\sigma \rrbracket \|_{\partial T}^2 \right)^{\frac{1}{2}} \end{aligned} \quad (78)$$

and due to the projection properties, there holds

$$\begin{aligned} & \left(\sum_{T \in \mathcal{T}} \frac{2}{\alpha} \| \Pi \sigma \cdot \mathbf{n} - \sigma \cdot \mathbf{n} \|_{\partial T}^2 + 2\alpha \| \Pi u - u \|_{\partial T}^2 + \beta \| \Pi \sigma \cdot \mathbf{n} - \sigma \cdot \mathbf{n} \|_{\partial T}^2 \right)^{\frac{1}{2}} \\ & \leq C \left(\left(\frac{2}{\alpha} + \beta \right) h^{2s+1} \| \sigma \|_{s+1}^2 + 2\alpha h^{2t+1} \| u \|_{t+1}^2 \right)^{\frac{1}{2}}, \end{aligned} \quad (79)$$

which concludes the proof. \square

The previous result states optimal convergence rates for jumps. In the following step Theorem 8 is proven, similarly to [LCQ17, Lemma 4.3], by applying an Aubin-Nitsche trick with the right-hand side $f = e_u$.

Proof of Theorem 8. Using an Aubin-Nitsche technique for the adjoint problem and inserting projections Π and Π_F , as well as applying Lemma 13 and Lemma 16, yields

$$\begin{aligned} \| e_u \|_{\Omega}^2 &= B(e_\sigma, e_{\hat{\sigma}}, e_u, e_{\hat{u}}, \phi, \phi_{\mathbf{n}}, w, w) \\ &= B(e_\sigma, e_{\hat{\sigma}}, e_u, e_{\hat{u}}, \phi - \Pi \phi, \phi_{\mathbf{n}} - \Pi_F \phi_{\mathbf{n}}, w - \Pi w, w - \Pi_F w) \\ &\quad + B(e_\sigma, e_{\hat{\sigma}}, e_u, e_{\hat{u}}, \Pi \phi, \Pi_F \phi_{\mathbf{n}}, \Pi w, \Pi_F w) \\ &= \sum_{T \in \mathcal{T}} ([e_u], (\phi - \Pi \phi) \cdot \mathbf{n})_{\partial T} - \alpha ([e_u], w - \Pi w)_{\partial T} + \beta (\llbracket e_\sigma \rrbracket, (\phi - \Pi \phi) \cdot \mathbf{n})_{\partial T} \\ &\quad + \sum_{T \in \mathcal{T}} (\Pi \sigma \cdot \mathbf{n} - \sigma \cdot \mathbf{n}, [\Pi w])_{\partial T} - \alpha (\Pi u - u, [\Pi w])_{\partial T} + \beta (\Pi \sigma \cdot \mathbf{n} - \sigma \cdot \mathbf{n}, \llbracket \Pi \phi \rrbracket)_{\partial T}. \end{aligned} \quad (80)$$

Estimating the terms leads to

$$\begin{aligned} & \| e_u \|_{\Omega}^2 \\ & \leq \left(\sum_{T \in \mathcal{T}} \alpha \| [e_u] \|_{\partial T}^2 + \beta \| \llbracket e_\sigma \rrbracket \|_{\partial T}^2 \right)^{\frac{1}{2}} \left(\sum_{T \in \mathcal{T}} \frac{2}{\alpha} \| (\phi - \Pi \phi) \cdot \mathbf{n} \|_{\partial T}^2 + 2\alpha \| w - \Pi w \|_{\partial T}^2 + \beta \| (\phi - \Pi \phi) \cdot \mathbf{n} \|_{\partial T}^2 \right)^{\frac{1}{2}} \\ & \quad + \left(\sum_{T \in \mathcal{T}} \frac{2}{\alpha} \| (\sigma - \Pi \sigma) \cdot \mathbf{n} \|_{\partial T}^2 + 2\alpha \| u - \Pi u \|_{\partial T}^2 + \beta \| (\sigma - \Pi \sigma) \cdot \mathbf{n} \|_{\partial T}^2 \right)^{\frac{1}{2}} \left(\sum_{T \in \mathcal{T}} \alpha \| [\Pi w] \|_{\partial T}^2 + \beta \| \llbracket \Pi \phi \rrbracket \|_{\partial T}^2 \right)^{\frac{1}{2}} \\ & \leq C \left(\left(\frac{2}{\alpha} + \beta \right) h^{2s+1} \| \sigma \|_{s+1}^2 + 2\alpha h^{2t+1} \| u \|_{t+1}^2 \right)^{\frac{1}{2}} \left(\left(\frac{2}{\alpha} + \beta \right) h^{2p+1} \| \phi \|_{p+1}^2 + 2\alpha h^{2q+1} \| w \|_{q+1}^2 \right)^{\frac{1}{2}}. \end{aligned} \quad (81)$$

The H^2 regularity of the adjoint problem implies $p = 0, q = 1$ giving

$$\| e_u \|_{\Omega} \leq C \left(\left(\frac{2}{\alpha} + \beta \right) (1 + \kappa)^2 h + 2\alpha (1 + \kappa)^2 \kappa^2 h^3 \right)^{\frac{1}{2}} \left(\left(\frac{2}{\alpha} + \beta \right) h^{2s+1} \| \sigma \|_{s+1}^2 + 2\alpha h^{2t+1} \| u \|_{t+1}^2 \right)^{\frac{1}{2}}, \quad (82)$$

which concludes the proof. \square

The applied Aubin-Nitsche technique is commonly used to prove the superconvergence of the projected error e_u . This is not the case for the presented HDG formulation, because the additional rate, generated due to the reasoning of the adjoint regularity, compensates for the otherwise sub-optimal rate through estimating boundary by volume terms.

5 Error Estimate for the Flux

To prove optimal convergence rates for the flux the issue due to h -independent stabilisation needs to be overcome. In [CGS10] a method based upon a specially devised projection is established and in [GM11] this method is applied to an HDG formulation of the Helmholtz equation to asymptotically show optimal rates. Removing the second facet variable $\hat{\sigma}_{\mathbf{n}}$ and the β -stabilisation in (16) would lead to the formulation therein. Therefore, similar steps as in [GM11] lead to the desired result, but they differ due to the β -stabilisation. For $\beta = 0$ the projection introduced in this work falls back to the projection in [CGS10].

To establish the needed projection it is favourable to eliminate the facet variables $\hat{\sigma}_{\mathbf{n}}$ and \hat{u} which results in an equivalent DG formulation. To accommodate the elimination of facet variables DG-jumps will be defined.

Lemma 17. *The discrete facet variables $\hat{\sigma}_{\mathbf{n},h}$ and \hat{u}_h of the solution of (16) are uniquely defined by*

$$\hat{\sigma}_{\mathbf{n}\pm,h} = \{\sigma_h\}_{\mathbf{n}\pm} := \frac{1}{2}(\sigma_{h,+} + \sigma_{h,-}) \cdot \mathbf{n}\pm \quad \text{on } F_{\Gamma}, \quad (83a)$$

$$\hat{\sigma}_{\mathbf{n},h} = \sigma_h \cdot \mathbf{n}, \quad \text{on } F_{\Omega} \quad (83b)$$

and

$$\hat{u}_h = \{u_h\} - \frac{1}{2\alpha}[\sigma_h]_{\mathbf{n}} := \frac{1}{2}(u_{h,+} + u_{h,-}) - \frac{1}{2\alpha}(\sigma_{h,+} \cdot \mathbf{n}_+ + \sigma_{h,-} \cdot \mathbf{n}_-) \quad \text{on } F_{\Gamma}, \quad (84a)$$

$$\hat{u}_h = \frac{1}{1+\alpha}(\Pi_{FG} - \sigma_h \cdot \mathbf{n} + \alpha u_h) \quad \text{on } F_{\Omega}. \quad (84b)$$

The same holds for the continuous facet variables $\hat{\sigma}_{\mathbf{n}\pm}$ and \hat{u} .

Proof. In the proof, the h -subscript for discrete variables is neglected. Combining $\hat{\tau}_{\mathbf{n}}$ terms on an inner facet F_{Γ} leads to

$$-\beta([\sigma]_{+}, \hat{\tau}_{\mathbf{n}+})_F - \beta([\sigma]_{-}, \hat{\tau}_{\mathbf{n}-})_F = -\beta(\sigma_{+} \cdot \mathbf{n}_{+} + \sigma_{-} \cdot \mathbf{n}_{-} - 2\hat{\sigma}_{\mathbf{n}+}, \hat{\tau}_{\mathbf{n}+})_F, \quad (85)$$

which directly implies (83a) and on outer facets F_{Ω} there holds

$$-\beta([\sigma], \hat{\tau}_{\mathbf{n}})_{\partial\Omega} = 0 \quad (86)$$

giving (83b). Similarly, for the scalar variable holds on inner facets

$$-((\sigma_{+} - \sigma_{-}) \cdot \mathbf{n}_{+} - \alpha(u_{+} + u_{-} - 2\hat{u}), \hat{v})_F = 0 \quad (87)$$

yielding (84a). Finally, the scalar variable on the domain boundary satisfies

$$-(\sigma \cdot \mathbf{n}, \hat{v})_{\partial\Omega} + \alpha(u - \hat{u}, \hat{v})_{\partial\Omega} - (\hat{u}, \hat{v})_{\partial\Omega} = -(g, \hat{v})_{\partial\Omega} \quad (88)$$

implying

$$(1 + \alpha)\hat{u} = \Pi_{FG} - \sigma \cdot \mathbf{n} + \alpha u. \quad (89)$$

□

With the previous lemma the facet variables can be eliminated from the HDG formulation and the volume variables satisfy the following DG formulation.

Lemma 18 (DG Formulation). *For given $g \in L^2(\partial\Omega)$ and $\kappa > 0$ find $\sigma \in H(\text{div}, \mathcal{T})$, $u \in L^2(\Omega)$, such that*

$$B_{DG}(\sigma, u, \tau, v) = \frac{1}{1+\alpha}(g, \tau \cdot \mathbf{n} - \alpha v)_{\partial\Omega} \quad (90)$$

holds for all $\tau \in H(\text{div}, \mathcal{T})$, $v \in L^2(\Omega)$ with $\alpha := 1$, $\beta := 1$ and the SLF

$$\begin{aligned} B_{DG}(\sigma, u, \tau, v) &:= \sum_{T \in \mathcal{T}} j\kappa(\sigma, \tau)_T + (u, \text{div } \tau)_T + (\text{div } \sigma, v)_T - j\kappa(u, v)_T \\ &+ \sum_{F_{\Gamma} \in \mathcal{F}} -(\{u\}, [\tau]_{\mathbf{n}})_{F_{\Gamma}} - ([\sigma]_{\mathbf{n}}, \{v\})_{F_{\Gamma}} - \frac{\alpha}{2}([u]_{+}, [v]_{+})_{F_{\Gamma}} + \left(\frac{1}{2\alpha} + \frac{\beta}{2}\right) ([\sigma]_{\mathbf{n}}, [\tau]_{\mathbf{n}})_{F_{\Gamma}} \\ &+ \frac{1}{1+\alpha} ((\sigma \cdot \mathbf{n}, \tau \cdot \mathbf{n})_{\partial\Omega} - \alpha((u, \tau \cdot \mathbf{n})_{\partial\Omega} + (\sigma \cdot \mathbf{n}, v)_{\partial\Omega} + (u, v)_{\partial\Omega})). \end{aligned} \quad (91)$$

The scalar jump on inner facets is defined as $[u]_{+} := u_{+} - u_{-}$.

Proof. With Lemma 17 the facet variables on inner facets are eliminated. Terms on adjacent elements are combined into DG form:

$$\beta([\![\sigma]\!]_+, \tau_+ \cdot \mathbf{n}_+)_{F_1} + \beta([\![\sigma]\!]_-, \tau_- \cdot \mathbf{n}_-)_{F_1} = \frac{\beta}{2}([\![\sigma]\!]_{\mathbf{n}}, [\![\tau]\!]_{\mathbf{n}})_{F_1}, \quad (92)$$

$$-(\hat{u}, [\![\tau]\!]_{\mathbf{n}})_{F_1} = -(\{u\} - \frac{1}{2\alpha}[\![\sigma]\!]_{\mathbf{n}}, [\![\tau]\!]_{\mathbf{n}})_{F_1}, \quad (93)$$

$$-\alpha([\![u]\!]_+, v_+)_{F_1} - \alpha([\![u]\!]_-, v_-)_{F_1} = -([\![\sigma]\!]_{\mathbf{n}}, \{v\})_{F_1} - \frac{\alpha}{2}([\![u]\!]_+, [v]_+)_{F_1}. \quad (94)$$

Replacing \hat{u} on the domain boundary leads to

$$\begin{aligned} -(\hat{u}, \tau \cdot \mathbf{n})_{\partial\Omega} - \alpha(u - \hat{u}, v)_{\partial\Omega} &= -\left(\frac{1}{1+\alpha}(g - \sigma \cdot \mathbf{n} + \alpha u), \tau \cdot \mathbf{n}\right)_{\partial\Omega} \\ &\quad - \alpha\left(u - \frac{1}{1+\alpha}(g - \sigma \cdot \mathbf{n} + \alpha u), v\right)_{\partial\Omega} \\ &= \frac{1}{1+\alpha}(\sigma \cdot \mathbf{n}, \tau \cdot \mathbf{n})_{\partial\Omega} - \frac{\alpha}{1+\alpha}(u, \tau \cdot \mathbf{n})_{\partial\Omega} - \frac{1}{1+\alpha}(g, \tau \cdot \mathbf{n})_{\partial\Omega} \\ &\quad - \alpha(u, v)_{\partial\Omega} - \frac{\alpha}{1+\alpha}(\sigma \cdot \mathbf{n}, v)_{\partial\Omega} + \frac{\alpha^2}{1+\alpha}(u, v)_{\partial\Omega} + \frac{\alpha}{1+\alpha}(g, v)_{\partial\Omega} \\ &= \frac{1}{1+\alpha}((\sigma \cdot \mathbf{n}, \tau \cdot \mathbf{n})_{\partial\Omega} - \alpha((u, \tau \cdot \mathbf{n})_{\partial\Omega} + (\sigma \cdot \mathbf{n}, v)_{\partial\Omega} + (u, v)_{\partial\Omega})) \\ &\quad - \frac{1}{1+\alpha}(g, \tau \cdot \mathbf{n} - \alpha v)_{\partial\Omega}. \end{aligned} \quad (95)$$

□

The next step towards an error bound for the flux is to introduce a suitable projection. The first result holds for general projections inserted into the DG formulation.

Lemma 19. *Let P be a projection*

$$P : (\sigma, u) \mapsto (P_\sigma(\sigma, u), P_u(\sigma, u)) \in \mathcal{RT}^p(\mathcal{T}) \times \mathcal{P}^p(\mathcal{T}) \quad (96)$$

into discrete spaces. With projected errors defined as

$$e_\sigma^P := P_\sigma(\sigma, u) - \sigma_h, \quad e_u^P := P_u(\sigma, u) - u_h, \quad (97)$$

there holds

$$\begin{aligned} \kappa \sum_{T \in \mathcal{T}} \|e_\sigma^P\|_T^2 &= -\Im \left(\sum_{T \in \mathcal{T}} j\kappa(\sigma - P_\sigma(\sigma, u), e_\sigma^P)_T + (u - P_u(\sigma, u), \operatorname{div} e_\sigma^P)_T \right. \\ &\quad \left. - (\sigma - P_\sigma(\sigma, u), \nabla e_u^P)_T - j\kappa(u - P_u(\sigma, u), e_u^P)_T - j\kappa \|e_u^P\|_T^2 \right) \\ &\quad - \Im \left(\sum_{F_1 \in \mathcal{F}} \left(\{\sigma - P_\sigma(\sigma, u)\}_{\mathbf{n}_+} - \frac{\alpha}{2}[u - P_u(\sigma, u)]_+, [e_u^P]_+ \right)_{F_1} \right. \\ &\quad \left. + \left(\left(\frac{1}{2\alpha} + \frac{\beta}{2} \right) [\sigma - P_\sigma(\sigma, u)]_{\mathbf{n}} - \{u - P_u(\sigma, u)\}, [e_\sigma^P]_{\mathbf{n}} \right)_{F_1} \right) \\ &\quad - \frac{1}{1+\alpha} \Im((\sigma - P_\sigma) \cdot \mathbf{n} - \alpha(u - P_u), e_\sigma^P \cdot \mathbf{n} + e_u^P)_{\partial\Omega}. \end{aligned} \quad (98)$$

Proof. The main idea is a repetition of the arguments in the proof of Lemma 13. To shorten the notation the arguments (σ, u) of $P_\sigma(\sigma, u)$ and $P_u(\sigma, u)$ will be omitted in the proof. Applying the Galerkin orthogonality and inserting the

projection yields

$$\begin{aligned}
 0 &= B_{DG}(\sigma - \sigma_h, u - u_h, u - \hat{u}_h, e_\sigma^P, e_u^P, e_{\hat{u}}) \\
 &= \sum_{T \in \mathcal{T}} j\kappa(\sigma - P_\sigma + e_\sigma^P, e_\sigma^P)_T + (u - P_u + e_u^P, \operatorname{div} e_\sigma^P)_T \\
 &\quad + (\operatorname{div}(\sigma - P_\sigma + e_\sigma^P), e_u^P)_T - j\kappa(u - P_u + e_u^P, e_u^P)_T \\
 &+ \sum_{F_1 \in \mathcal{F}} -(\{u - P_u + e_u^P\}, [e_\sigma^P]_{\mathbf{n}})_{F_1} - ([\sigma - P_\sigma + e_\sigma^P]_{\mathbf{n}}, \{e_u^P\})_{F_1} \\
 &\quad - \frac{\alpha}{2}([u - P_u + e_u^P]_+, [e_u^P]_+)_{F_1} + \left(\frac{1}{2\alpha} + \frac{\beta}{2}\right) ([\sigma - P_\sigma + e_\sigma^P]_{\mathbf{n}}, [e_\sigma^P]_{\mathbf{n}})_{F_1} \\
 &+ \frac{1}{1+\alpha} \left(((\sigma - P_\sigma + e_\sigma^P) \cdot \mathbf{n}, e_\sigma^P \cdot \mathbf{n})_{\partial\Omega} - \alpha(u - P_u + e_u^P, e_\sigma^P \cdot \mathbf{n})_{\partial\Omega} \right. \\
 &\quad \left. - \alpha((\sigma - P_\sigma + e_\sigma^P) \cdot \mathbf{n}, e_u^P)_{\partial\Omega} - \alpha(u - P_u + e_u^P, e_u^P)_{\partial\Omega} \right).
 \end{aligned} \tag{99}$$

For the volume terms there holds after partial integration

$$\begin{aligned}
 &\sum_{T \in \mathcal{T}} j\kappa(\sigma - P_\sigma + e_\sigma^P, e_\sigma^P)_T + (u - P_u + e_u^P, \operatorname{div} e_\sigma^P)_T \\
 &\quad + (\operatorname{div}(\sigma - P_\sigma + e_\sigma^P), e_u^P)_T - j\kappa(u - P_u + e_u^P, e_u^P)_T \\
 &= \sum_{T \in \mathcal{T}} j\kappa(\sigma - P_\sigma, e_\sigma^P)_T + j\kappa \|e_\sigma^P\|_T^2 + (u - P_u, \operatorname{div} e_\sigma^P)_T + 2\Re(e_u^P, \operatorname{div} e_\sigma^P)_T \\
 &\quad - (\sigma - P_\sigma, \nabla e_u^P)_T + ((\sigma - P_\sigma) \cdot \mathbf{n}, e_u^P)_{\partial T} - j\kappa(u - P_u, e_u^P)_T - j\kappa \|e_u^P\|_T^2
 \end{aligned} \tag{100}$$

and connecting the arising boundary terms on inner facets leads to

$$((\sigma - P_{\sigma,+}) \cdot \mathbf{n}_+, [e_{u,+}^P]_{F_1}) + ((\sigma - P_{\sigma,-}) \cdot \mathbf{n}_-, [e_{u,-}^P]_{F_1}) = (\{\sigma - P_\sigma\}_{\mathbf{n}_+}, [e_{u,+}^P]_{F_1}) + ([\sigma - P_\sigma]_{\mathbf{n}}, \{e_u^P\})_{F_1}. \tag{101}$$

Combining these with the facet terms in (99) results in

$$\begin{aligned}
 &\sum_{F_1 \in \mathcal{F}} -(\{u - P_u + e_u^P\}, [e_\sigma^P]_{\mathbf{n}})_{F_1} - ([\sigma - P_\sigma + e_\sigma^P]_{\mathbf{n}}, \{e_u^P\})_{F_1} \\
 &\quad - \frac{\alpha}{2}([u - P_u + e_u^P]_+, [e_u^P]_+)_{F_1} + \left(\frac{1}{2\alpha} + \frac{\beta}{2}\right) ([\sigma - P_\sigma + e_\sigma^P]_{\mathbf{n}}, [e_\sigma^P]_{\mathbf{n}})_{F_1} \\
 &\quad + (\{\sigma - P_\sigma\}_{\mathbf{n}_+}, [e_{u,+}^P]_{F_1}) + ([\sigma - P_\sigma]_{\mathbf{n}}, \{e_u^P\})_{F_1} \\
 &= \sum_{F_1 \in \mathcal{F}} -2\Re(\{e_u^P\}, [e_\sigma^P]_{\mathbf{n}})_{F_1} + \left(\{\sigma - P_\sigma\}_{\mathbf{n}_+} - \frac{\alpha}{2}[u - P_u]_+, [e_{u,+}^P]_{F_1}\right) - \frac{\alpha}{2} \| [e_{u,+}^P]_{F_1} \|_{F_1}^2 \\
 &\quad + \left(\left(\frac{1}{2\alpha} + \frac{\beta}{2}\right) [\sigma - P_\sigma]_{\mathbf{n}} - \{u - P_u\}, [e_\sigma^P]_{\mathbf{n}} \right)_{F_1} + \left(\frac{1}{2\alpha} + \frac{\beta}{2}\right) \| [e_\sigma^P]_{\mathbf{n}} \|_{F_1}^2.
 \end{aligned} \tag{102}$$

Finally, on the domain boundary there holds, considering the additional term arising from partial integration,

$$\begin{aligned}
 &\frac{1}{1+\alpha} \left(((\sigma - P_\sigma + e_\sigma^P) \cdot \mathbf{n}, e_\sigma^P \cdot \mathbf{n})_{\partial\Omega} - \alpha(u - P_u + e_u^P, e_\sigma^P \cdot \mathbf{n})_{\partial\Omega} \right. \\
 &\quad \left. - \alpha((\sigma - P_\sigma + e_\sigma^P) \cdot \mathbf{n}, e_u^P)_{\partial\Omega} - \alpha(u - P_u + e_u^P, e_u^P)_{\partial\Omega} \right) + ((\sigma - P_\sigma) \cdot \mathbf{n}, e_u^P)_{\partial\Omega} \\
 &= \frac{1}{1+\alpha} \left(((\sigma - P_\sigma) \cdot \mathbf{n}, e_\sigma^P \cdot \mathbf{n})_{\partial\Omega} + \|e_\sigma^P \cdot \mathbf{n}\|_{\partial\Omega}^2 - \alpha(u - P_u, e_\sigma^P \cdot \mathbf{n})_{\partial\Omega} - 2\alpha\Re(e_u^P, e_\sigma^P \cdot \mathbf{n})_{\partial\Omega} \right. \\
 &\quad \left. + ((\sigma - P_\sigma) \cdot \mathbf{n}, e_u^P)_{\partial\Omega} - \alpha(u - P_u, e_u^P)_{\partial\Omega} - \alpha \|e_u^P\|_{\partial\Omega}^2 \right) \\
 &= \frac{1}{1+\alpha} \left(((\sigma - P_\sigma) \cdot \mathbf{n} - \alpha(u - P_u), e_\sigma^P \cdot \mathbf{n})_{\partial\Omega} + \|e_\sigma^P \cdot \mathbf{n}\|_{\partial\Omega}^2 - 2\alpha\Re(e_u^P, e_\sigma^P \cdot \mathbf{n})_{\partial\Omega} \right. \\
 &\quad \left. + ((\sigma - P_\sigma) \cdot \mathbf{n} - \alpha(u - P_u), e_u^P)_{\partial\Omega} - \alpha \|e_u^P\|_{\partial\Omega}^2 \right) \\
 &= \frac{1}{1+\alpha} \left(((\sigma - P_\sigma) \cdot \mathbf{n} - \alpha(u - P_u), e_\sigma^P \cdot \mathbf{n} + e_u^P)_{\partial\Omega} + \|e_\sigma^P \cdot \mathbf{n}\|_{\partial\Omega}^2 - 2\alpha\Re(e_u^P, e_\sigma^P \cdot \mathbf{n})_{\partial\Omega} - \alpha \|e_u^P\|_{\partial\Omega}^2 \right).
 \end{aligned} \tag{103}$$

Taking the imaginary part implies

$$0 = \Im B_{DG}(\sigma - \sigma_h, u - u_h, e_{\bar{u}}, e_{\sigma}^P, e_u^P, e_{\bar{u}}) \quad (104)$$

$$= \Im \sum_{T \in \mathcal{T}} j\kappa(\sigma - P_{\sigma}, e_{\sigma}^P)_T + j\kappa \|e_{\sigma}^P\|_T^2 + (u - P_u, \operatorname{div} e_{\sigma}^P)_T \quad (105)$$

$$- (\sigma - P_{\sigma}, \nabla e_u^P)_T - j\kappa(u - P_u, e_u^P)_T - j\kappa \|e_u^P\|_T^2 \quad (106)$$

$$+ \Im \sum_{F_1 \in \mathcal{F}} \left(\{\sigma - P_{\sigma}\}_{\mathbf{n}_+} - \frac{\alpha}{2}[u - P_u]_+, [e_u^P]_+ \right)_{F_1} \quad (107)$$

$$+ \left(\left(\frac{1}{2\alpha} + \frac{\beta}{2} \right) [\sigma - P_{\sigma}]_{\mathbf{n}} - \{u - P_u\}, [e_{\sigma}^P]_{\mathbf{n}} \right)_{F_1} \quad (108)$$

$$+ \frac{1}{1 + \alpha} \Im((\sigma - P_{\sigma}) \cdot \mathbf{n} - \alpha(u - P_u), e_{\sigma}^P \cdot \mathbf{n} + e_u^P)_{\partial\Omega}, \quad (109)$$

which concludes the proof. \square

From the previous lemma, it can be seen that a suitable projection for vanishing facet terms needs to satisfy

$$\left(\{\sigma - P_{\sigma}\}_{\mathbf{n}_+} - \frac{\alpha}{2}[u - P_u]_+, \mu_h \right)_{F_1} = 0 \quad \forall \mu_h \in \mathcal{P}^p(F_1), \quad (110)$$

$$\left(\left(\frac{1}{2\alpha} + \frac{\beta}{2} \right) [\sigma - P_{\sigma}]_{\mathbf{n}} - \{u - P_u\}, \nu_h \right)_{F_1} = 0 \quad \forall \nu_h \in \mathcal{P}^p(F_1), \quad (111)$$

on inner facets. The two conditions per facet can be reformulated into the following equivalent form

$$\left(\frac{1}{\alpha} + \beta \right) ((\sigma - P_{\sigma,+}) \cdot \mathbf{n}_+, \mu_h)_{F_1} = (u - P_{u,+}, \mu_h)_{F_1} + \frac{\alpha\beta}{2} ([u - P_u]_+, \mu_h)_{F_1}, \quad (112)$$

$$\left(\frac{1}{\alpha} + \beta \right) ((\sigma - P_{\sigma,-}) \cdot \mathbf{n}_-, \nu_h)_{F_1} = (u - P_{u,-}, \nu_h)_{F_1} + \frac{\alpha\beta}{2} ([u - P_u]_-, \nu_h)_{F_1}. \quad (113)$$

Without a β -stabilisation this would exactly be the projection in [CGS10, GM11, Say13]. Collecting all required properties of the projection looks as follows.

Definition 20. Let P be the projection

$$P : (\sigma, u) \mapsto (P_{\sigma}(\sigma, u), P_u(\sigma, u)) \in \mathcal{RT}^p(\mathcal{T}) \times \mathcal{P}^p(\mathcal{T}) \quad (114)$$

defined by

$$(P_{\sigma}(\sigma, u), \tau_h)_T = (\sigma, \tau_h)_T \quad \forall \tau_h \in [\mathcal{P}^{p-1}(T)]^d, \quad (115a)$$

$$(P_u(\sigma, u), v_h)_T = (u, v_h)_T \quad \forall v_h \in \mathcal{P}^p(T), \quad (115b)$$

$$\left(\frac{1}{2\alpha} + \frac{\beta}{2} \right) ([\sigma - P_{\sigma}]_+, \mu_h)_{F_1} = (\{u - P_u\}, \mu_h)_{F_1} \quad \forall \mu_h \in \mathcal{P}^p(F_1), \quad (115c)$$

$$(\{\sigma - P_{\sigma}\}_+, \mu_h)_{F_1} = \frac{\alpha}{2} ([u - P_u]_+, \mu_h)_{F_1} \quad \forall \mu_h \in \mathcal{P}^p(F_1), \quad (115d)$$

$$(\sigma \cdot \mathbf{n} - P_{\sigma} \cdot \mathbf{n}, \mu_h)_{F_O} = \alpha(u - P_u, \mu_h)_{F_O} \quad \forall \mu_h \in \mathcal{P}^p(F_O). \quad (115e)$$

On the domain boundary, the projection has to have the same properties as the projection in [CGS10]. For P existence and uniqueness, as well as the projection property and a suitable approximation property need to be proven. The definition represents a square linear system of equations, therefore uniqueness of the projection automatically implies its existence.

The projection P_u is decoupled from σ . The properties for P_u are proven in the following lemma.

Lemma 21 (Projection Decoupling). *The projection P_u is uniquely defined by*

$$(P_u(\sigma, u), v_h)_T = (u, v_h)_T \quad \forall v_h \in \mathcal{P}^p(T) \quad (116)$$

and only depends on u , therefore $P_u(\sigma, u) = P_u(u)$. For $u \in H^{p+1}(T)$ there holds

$$\|u - P_u(u)\|_T \leq Ch^{p+1}|u|_{H^{p+1}(T)}, \quad (117)$$

with a constant $C > 0$ independent of h, κ, α, β .

Proof. Equation (115b) implies that $P_u(\sigma, u)$ is the L^2 -projection Πu . \square

The proof for P_σ is more involved and similar to the analysis in [CGS10, Say13].

Lemma 22. *The space $\mathcal{P}_\perp^p(T)$ is defined by*

$$\mathcal{P}_\perp^p(T) := \{u \in \mathcal{P}^p(T) : (u, v)_T = 0, \forall v \in \mathcal{P}^{p-1}(T)\}. \quad (118)$$

If $u \in \mathcal{P}_\perp^p(T)$ satisfies $u = 0$ on a facet of T then $u \equiv 0$ on the whole element.

Proof. See [CGS10, Lemma A.1] and [Say13, Lemma 2.1]. \square

Lemma 23. *The space $\mathcal{RT}_\perp^p(T)$ is defined by*

$$\mathcal{RT}_\perp^p(T) := \{\sigma \in \mathcal{RT}^p(T) : (\sigma, \tau)_T = 0, \forall \tau \in [\mathcal{P}^{p-1}(T)]^d\}. \quad (119)$$

Assume $\sigma \in \mathcal{RT}_\perp^p(T)$ then there holds

$$\|\sigma\|_T \leq Ch^{\frac{1}{2}} \|\sigma \cdot \mathbf{n}\|_{\partial T}, \quad (120)$$

with a constant $C > 0$ independent of h, κ, α, β .

Proof. The proof is similar to [CGS10, Proposition A.3] and [Say13, Lemma 2.1]. First, it is shown that the boundary term is a norm on the space $\mathcal{RT}_\perp^p(T)$. Assuming $\sigma \cdot \mathbf{n} = 0$ on ∂T then there holds

$$\|\operatorname{div} \sigma\|_T^2 = (\sigma \cdot \mathbf{n}, \operatorname{div} \sigma)_{\partial T} - (\sigma, \nabla \operatorname{div} \sigma)_T = 0, \quad (121)$$

because $\nabla \operatorname{div} \sigma \in [\mathcal{P}^{p-1}(T)]^d$. According to [Say13, Proposition 2.3] this implies $\sigma \in [\mathcal{P}^p(T)]^d$ and by splitting σ into

$$\sigma = \sum_{i=1}^{d-1} \sigma \cdot \mathbf{n}_i \quad (122)$$

there holds $\sigma \cdot \mathbf{n}_i \in \mathcal{P}_\perp^p(T)$ as well as $\sigma \cdot \mathbf{n}_i = 0$ on the facet F_1 . Then Lemma 22 implies that $\sigma \cdot \mathbf{n}_i$ vanishes on the whole element and therefore $\sigma = 0$. The estimate is proven by a standard scaling argument. \square

With this lemma, the uniqueness and approximation property of P_σ can be proven.

Lemma 24. *Assuming H^{p+1} -regularity of σ and u , there exists a constant $C > 0$, independent of κ, h, α, β , so that*

$$\|\sigma - P_\sigma(\sigma, u)\|_\Omega \leq Ch^{p+1} \left(|\sigma|_{H^{p+1}} + \frac{1 + \alpha\beta}{\alpha^{-1} + \beta} |u|_{H^{p+1}} \right). \quad (123)$$

Proof. The proof is an adaptation of the approach in [CGS10, Proposition A.3]. Consider the standard \mathcal{RT} -interpolant satisfying

$$(\mathcal{RT}(\sigma), \tau_h)_T = (\sigma, \tau_h)_T \quad \forall \tau_h \in [\mathcal{P}^{p-1}(T)]^d, \quad (124a)$$

$$((\sigma - \mathcal{RT}(\sigma)) \cdot \mathbf{n}, \mu_h)_F = 0 \quad \forall \mu_h \in \mathcal{P}^p(F) \quad (124b)$$

and define $\delta_\sigma := \mathcal{RT}(\sigma) - P_\sigma(\sigma, u)$. Due to (115a) and (115c - 115e) there holds for δ_σ

$$(\delta_\sigma, \tau_h)_T = 0 \quad \forall \tau_h \in [\mathcal{P}^{p-1}(T)]^d, \quad (125)$$

$$\left(\frac{1}{\alpha} + \beta \right) (\delta_\sigma \cdot \mathbf{n}, \mu_h)_{\partial T \cap F_1} = (u - P_u, \mu_h)_{\partial T \cap F_1} + \frac{\alpha\beta}{2} ([u - P_u], \mu_h)_{\partial T \cap F_1} \quad \forall \mu_h \in \mathcal{P}^p(F_1), \quad (126)$$

$$\left(\frac{1}{\alpha} + \beta \right) (\delta_\sigma \cdot \mathbf{n}, \mu_h)_{\partial T \cap F_0} = (1 + \alpha\beta)(u - P_u, \mu_h)_{\partial T \cap F_0} \quad \forall \mu_h \in \mathcal{P}^p(F_0). \quad (127)$$

The idea is to choose $\mu_h = \delta_\sigma \cdot \mathbf{n}$ in the equations above and to estimate facet terms by

$$\begin{aligned} |(u - P_u, \delta_\sigma \cdot \mathbf{n})_F| &\leq Ch^{-\frac{1}{2}} \|u - P_u\|_F \|\delta_\sigma\|_T \\ &\leq Ch^{-1} (\|u - P_u\|_T + h|u - P_u|_{H^1(T)}) \|\delta_\sigma\|_T \\ &\leq Ch^p |u|_{H^{p+1}} \|\delta_\sigma\|_T. \end{aligned} \quad (128)$$

The constant C changes in each line, but stays independent of h, κ, α, β . Due to (125) Lemma 23 can be applied yielding

$$\begin{aligned}
 \left(\frac{1}{\alpha} + \beta\right) \|\delta_\sigma\|_T^2 &\leq \left(\frac{1}{\alpha} + \beta\right) Ch \|\delta_\sigma \cdot \mathbf{n}\|_{\partial T}^2 \\
 &= Ch \left((u - P_u, \delta_\sigma \cdot \mathbf{n})_{\partial T \setminus \partial \Omega} + \frac{\alpha\beta}{2} ([u - P_u], \delta_\sigma \cdot \mathbf{n})_{\partial T \setminus \partial \Omega} \right. \\
 &\quad \left. + (1 + \alpha\beta)(u - P_u, \delta_\sigma \cdot \mathbf{n})_{\partial T \cap \partial \Omega} \right) \\
 &\leq C(1 + \alpha\beta)h^{p+1}|u|_{H^{p+1}} \|\delta_\sigma\|_T,
 \end{aligned} \tag{129}$$

which implies

$$\|\delta_\sigma\|_T \leq C \frac{1 + \alpha\beta}{\alpha^{-1} + \beta} h^{p+1} |u|_{H^{p+1}} \tag{130}$$

and finally gives

$$\begin{aligned}
 \|\sigma - P_\sigma(\sigma, u)\|_\Omega &\leq \|\sigma - \mathcal{RT}(\sigma)\|_\Omega + \|\delta_\sigma\|_\Omega \\
 &\leq Ch^{p+1} \left(|\sigma|_{H^{p+1}} + \frac{1 + \alpha\beta}{\alpha^{-1} + \beta} |u|_{H^{p+1}} \right).
 \end{aligned} \tag{131}$$

□

With this result, the error estimate for the flux can be finalised.

Proof of Theorem 9. According to Lemma 19 in combination with the projection in Definition 20 there holds

$$\begin{aligned}
 \kappa \sum_{T \in \mathcal{T}} \|e_\sigma^P\|_T^2 &= -\Im \left(\sum_{T \in \mathcal{T}} j\kappa (\sigma - P_\sigma(\sigma, u), e_\sigma^P)_T - j\kappa \|e_u^P\|_T^2 \right) \\
 &\leq \kappa \sum_{T \in \mathcal{T}} |(\sigma - P_\sigma(\sigma, u), e_\sigma^P)_T| + \|e_u^P\|_T^2 \\
 &\leq \kappa \sum_{T \in \mathcal{T}} \|\sigma - P_\sigma(\sigma, u)\|_T \|e_\sigma^P\|_T + \|e_u^P\|_T^2.
 \end{aligned} \tag{132}$$

Applying Young's inequality, Lemma 24 for $\sigma - P_\sigma$ and Theorem 8 for e_u^P yields

$$\begin{aligned}
 \kappa \sum_{T \in \mathcal{T}} \|e_\sigma^P\|_T^2 &\leq \kappa \sum_{T \in \mathcal{T}} \|\sigma - P_\sigma(\sigma, u)\|_T^2 + 2\|e_u^P\|_T^2 \\
 &\leq \kappa Ch^{2p+2} \left(\|\sigma\|_{H^{p+1}}^2 + \left(\frac{1 + \alpha\beta}{\alpha^{-1} + \beta}\right)^2 \|u\|_{H^{p+1}}^2 \right) \\
 &\quad + \kappa Ch^{2p+2} \left(\left(\frac{2}{\alpha} + \beta\right) (1 + \kappa)^2 + 2\alpha(1 + \kappa)^2 \kappa^2 h^2 \right) \left(\left(\frac{2}{\alpha} + \beta\right) \|\sigma\|_{H^{p+1}}^2 + 2\alpha \|u\|_{H^{p+1}}^2 \right).
 \end{aligned} \tag{133}$$

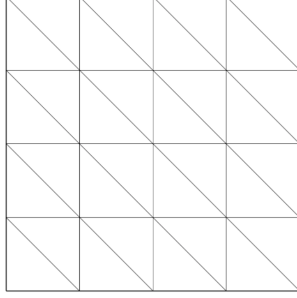
Considering

$$\|\sigma - \sigma_h\|_\Omega \leq \|\sigma - P_\sigma(\sigma, u)\|_\Omega + \|e_\sigma^P\|_\Omega \tag{134}$$

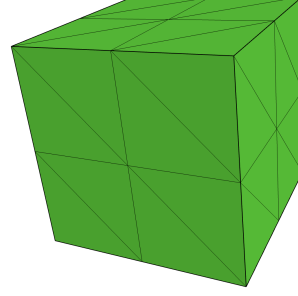
and applying Lemma 24 concludes the proof. □

6 Numerical Experiments

The mixed Helmholtz problem (16) has been discretised with the open source FE software NETGEN/NGSolve [Sch97, Sch14]. It provides the required high-order FE spaces as well as the tools for the iterative solver. First, the established error estimates are probed by simulations on convex domains with plane waves as analytical solutions.



(a) The 2D structured mesh of the unit square is shown for the choice of $N = 4$.



(b) The 3D structured mesh of the unit cube is shown for the choice of $N = 2$.

Figure 1: The structured meshes for the plane wave simulations in 2D and 3D are visualised.

6.1 2D Plane Wave

A 2D plane wave example has been considered on the square domain $\Omega = (0, 1)^2$ discretised by a structured mesh comprised of triangles. For fixed $N \in \mathbb{N}_+$ the domain has been split into $N \times N$ identical squares and each smaller square was split into two triangles by a line from the top left to the bottom right corner. In Figure 1a the mesh for $N = 4$ is shown. The excitation g in the HDG formulation (16) has been chosen so that the analytical solution is the plane wave

$$u(x, y) = e^{j\kappa(x \cos \theta + y \sin \theta)} \quad (135)$$

with an angle of $\theta = \pi/6$. The wave number was fixed at $\kappa = 5$ and structured meshes corresponding to $N = \{2, 4, 8, 16, 32, 64, 128\}$ have been considered. In Figure 3 the convergence rates for the polynomial degrees $p = \{0, 1, 2, 3\}$ with respect to the mesh size are visualised. In alignment with the established theory in Section 4 the projected error $e_u = \Pi u - u_h$ converges at a rate of h^{p+1} .

6.2 3D Plane Wave

Similarly to the previous 2D example, a 3D plane wave simulation has been considered on the cubic domain $\Omega = (0, 1)^3$ discretised with a structured mesh comprised of tetrahedra. For fixed $N \in \mathbb{N}_+$ the domain has been split into $N \times N \times N$ identical cubes and each smaller cube was split into six tetrahedra. In Figure 1b the mesh for $N = 2$ is shown. The excitation g in the HDG formulation (16) has been chosen so that the analytical solution is the plane wave

$$u(x, y, z) = e^{j\kappa(x \cos \theta + (y \cos \eta + z \sin \eta) \sin \theta)} \quad (136)$$

with the angles $\theta = \pi/6$ and $\eta = \pi/5$. The wave number was fixed at $\kappa = 3$ and a sequence of structured meshes corresponding to $N = \{2, 6, 10, 14, 18, 22, 26\}$ has been considered. In Figure 3 the convergence rates for the polynomial degrees $p = \{0, 1\}$ with respect to the mesh size are visualised.

For the following larger simulations, static condensation was applied eliminating the volume variables σ_h and u_h . A system of linear equations for the facet variables $\hat{\sigma}_{\mathbf{n},h}$ and \hat{u}_h remained to be solved and the solution was afterwards extended back to the interior of elements. As an iterative solver a BiCGSTAB with a block Gauss-Seidel preconditioner and a tolerance of $\varepsilon = 10^{-5}$ was applied. In 2D simulations, the facet variables in a vertex patch were combined into blocks and for 3D simulations, facet-wise blocks were generated.

6.3 Heterogeneous Materials

The analysis in this work only covers the case of constant material parameters, but the method can also cope with heterogeneous materials. In this numerical experiment, the following heterogeneous Helmholtz problem has been considered.

Definition 25 (Mixed Heterogeneous Helmholtz Problem). For given $\kappa > 0$ and $g \in L^2(\partial\Omega)$, let (σ, u) be the solution of the boundary value problem (BVP)

$$j\kappa\sigma - \nabla u = 0 \quad \text{in } \Omega, \quad (137a)$$

$$-\operatorname{div} \sigma + j\kappa c u = 0 \quad \text{in } \Omega, \quad (137b)$$

$$\sigma \cdot \mathbf{n} + u = g \quad \text{on } \partial\Omega, \quad (137c)$$

where $c(\mathbf{x}) > 0$ is a given positive, bounded, varying material coefficient.

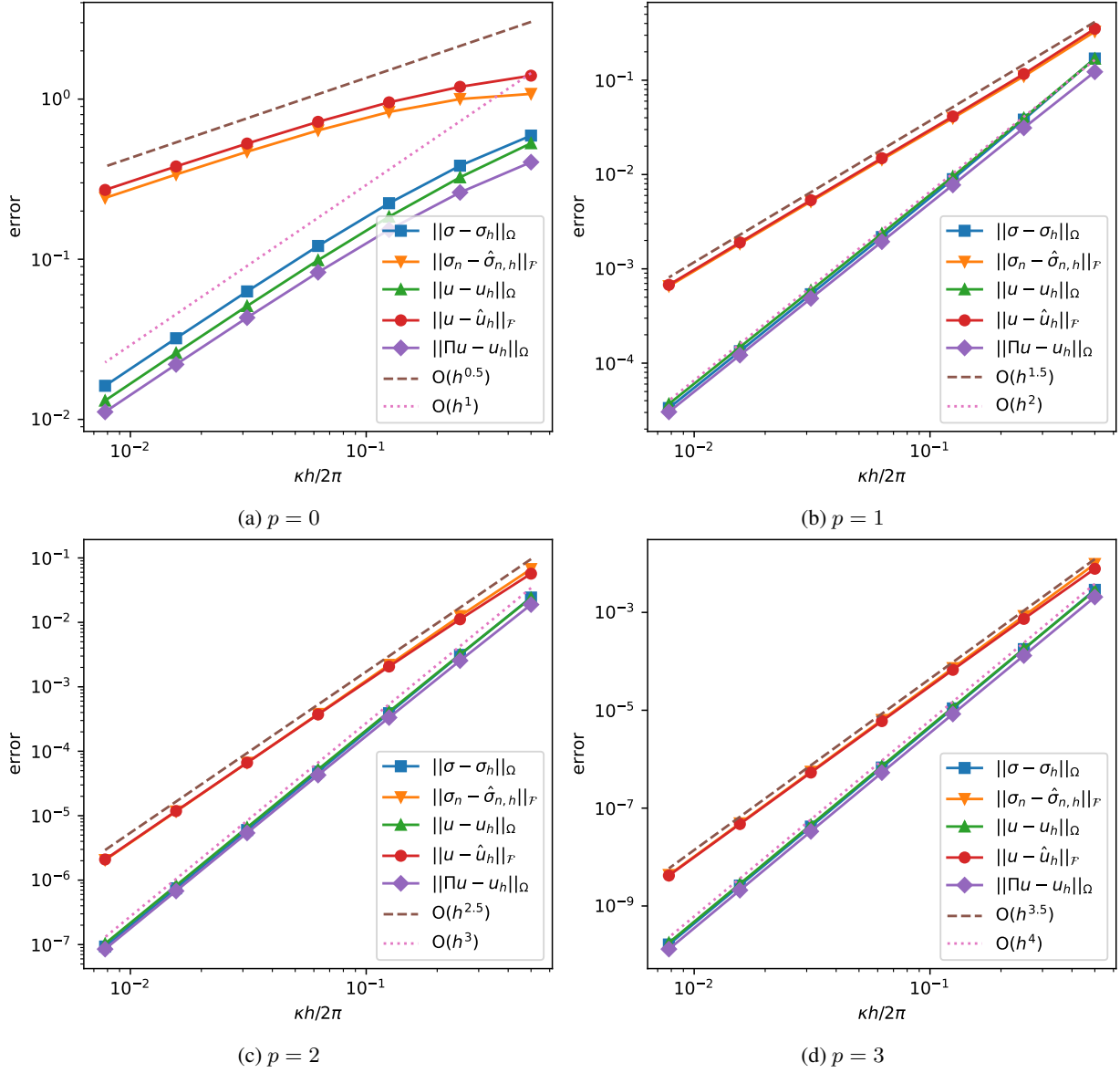


Figure 2: The convergence of the 2D plane wave example on a sequence of structured meshes for various polynomial degrees is visualised. A convergence rate of h^{p+1} can be seen for pressure, flux and the projected error $\Pi u - u_h$. The facet variables $\hat{\sigma}_{n,h}$ and \hat{u}_h converge with a rate of $h^{p+1/2}$.

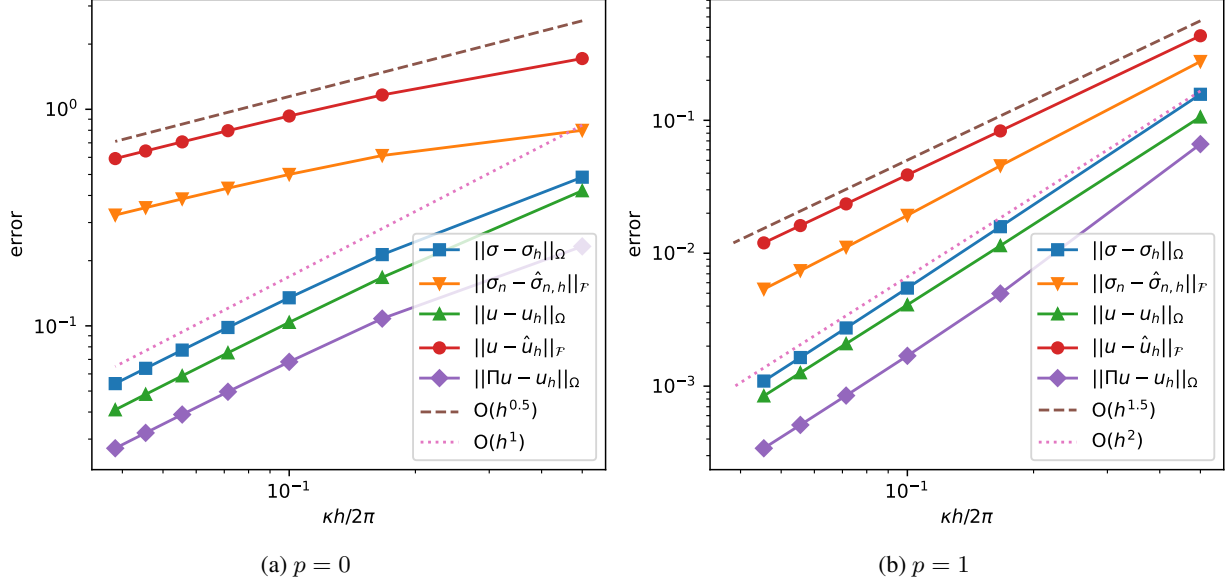


Figure 3: The convergence of the 3D plane wave example on a sequence of structured meshes for polynomial degrees zero and one is visualised. A convergence rate of h^{p+1} can be seen for pressure, flux and the projected error $\Pi u - u_h$. The facet variables $\hat{\sigma}_{n,h}$ and \hat{u}_h converge with a rate of $h^{p+1/2}$.

Table 1: NDoF for the 2D simulation with heterogeneous materials

	σ_h	$\hat{\sigma}_{n,h}$	u_h	\hat{u}_h
NDoFs	4 279 920	1 072 530	2 139 960	1 072 530

The following 2D-examples have similar geometry and material coefficients as [GGS20, Experiment 6.5]. The domain consists of the square $\Omega = (-1, 1)^2$ with a circle of radius $r = 1/2$ as a penetrable obstacle centred in the middle. The wavenumber has been chosen as $\kappa = 100$ and the excitation was

$$g(\mathbf{x}) = -10j\kappa e^{-20(y + \frac{1}{10})^2} \quad (138)$$

on the left boundary. On the other outer boundaries, homogenous Robin boundary conditions were applied. The excitation is slightly offset from the axis of symmetry and represents an inflowing Gaussian peak. For the discrete FE spaces, a polynomial degree of $p = 4$ has been used and the maximal mesh size was chosen as $h = 2\pi/8\kappa$. Two different material profiles were considered for the simulations, specifically

$$c_1(\mathbf{x}) := \begin{cases} 2\sqrt{x^2 + y^2}c_{min} + (1 - 2\sqrt{x^2 + y^2})c_{max}, & \|\mathbf{x}\|_2 < \frac{1}{2}, \\ 1, & \text{otherwise,} \end{cases} \quad (139)$$

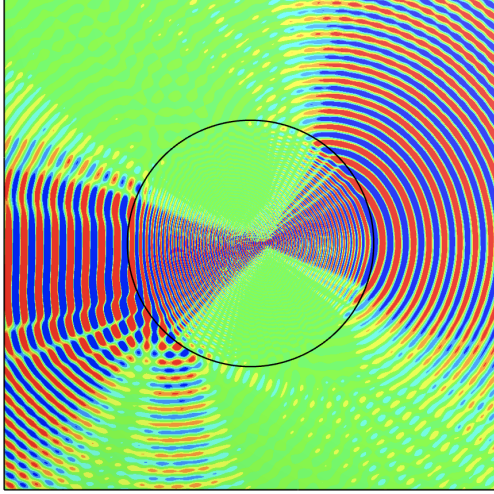
and

$$c_2(\mathbf{x}) := \begin{cases} (1 - 2\sqrt{x^2 + y^2})c_{min} + 2\sqrt{x^2 + y^2}c_{max}, & \|\mathbf{x}\|_2 < \frac{1}{2}, \\ 1, & \text{otherwise,} \end{cases} \quad (140)$$

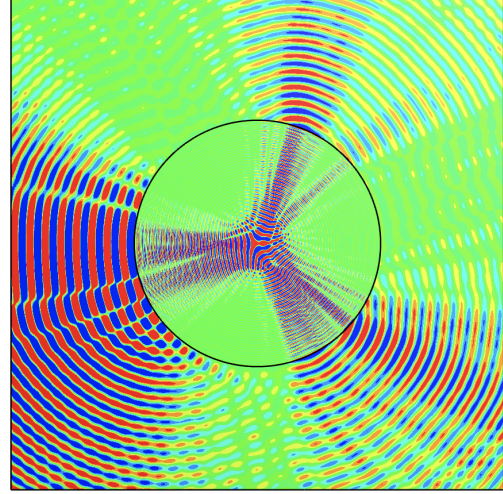
with the minimum $c_{min} = 0.02$ and the maximum $c_{max} = 50$. The first material c_1 is constant outside the circle and decreases linearly with respect to the radius. Contrary, the second material c_2 increases linearly. In Figure 4a and 4b the real part of the pressure can be seen for the simulations with material coefficients c_1 and c_2 . Both simulations have been carried out on 8 cores, required approximately 14 GB of memory and the number of degrees of freedom (NDoF) can be found in Table 1. After static condensation a system of linear equations with the combined size of $\hat{\sigma}_{n,h}$ and \hat{u}_h was solved. In Table 2 the iteration counts and the computation times for both simulations are shown. The wall time reflects the duration of the iterative solve and the processor time is the sum of the computation times of all cores combined.

6.4 Scattering on Spheres

A 3D example with 100 spheres as scatterers treated as homogeneous Dirichlet boundaries has been considered. The domain is comprised of the cube $\Omega = (0, 1)^3$ and on the plane of symmetry perpendicular to the x -axis an array of



(a) Result for linearly decreasing material c_1 with respect to the radius inside the circle



(b) Result for linearly increasing material c_2 with respect to the radius inside the circle

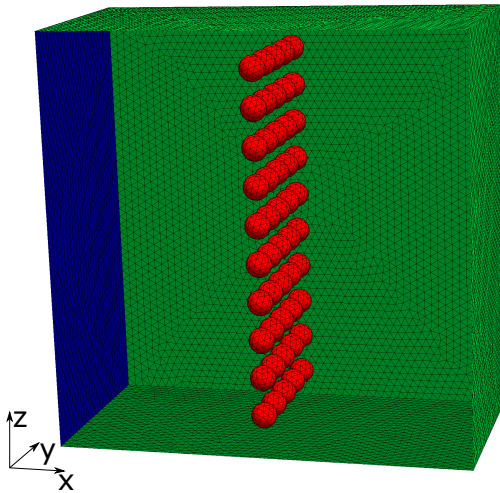
Figure 4: The real part $\Re(u_h)$ of the pressure is shown for simulations with the heterogeneous material coefficients c_1 and c_2 . A Gaussian peak has been applied on the left boundary as an excitation.

Table 2: Number of iterations and computation times for heterogeneous materials

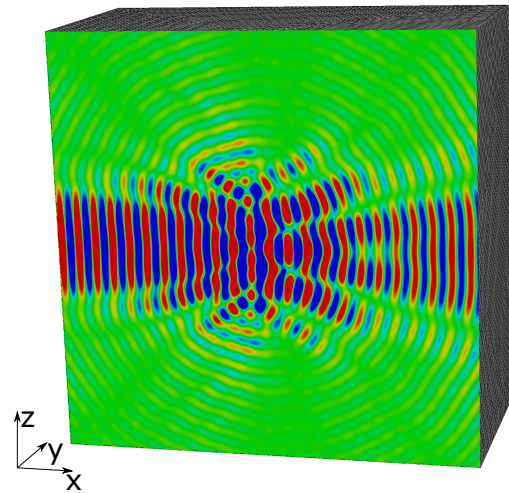
	iterations	wall time in s	processor time in s	processor time per core in s
c_1	5 833	2 363	15 712	1 964
c_2	4 024	1 634	10 867	1 359

the scatterers is positioned. They are aligned on a 10×10 grid with an equidistant spacing of $\delta = 1/11$ in between midpoints. The radius $r = \delta/3$ of each sphere is identical. A cut view of the geometry and the solution can be seen in Figure 5. A wavenumber of $\kappa = 150$ was considered and the material coefficient was constant $c = 1$. The excitation was the Gaussian peak

$$g(\mathbf{x}) = -10j\kappa e^{-100\left(\left(y-\frac{1}{2}\right)^2 + \left(z-\frac{1}{2}\right)^2\right)} \quad (141)$$



(a) The spherical scatterers can be seen in red and the left excitation boundary is in blue.



(b) The real part $\Re(u_h)$ of the pressure is drawn on the plane of symmetry.

Figure 5: A cut view along the x, z -plane of symmetry is shown for the 3D-example with spherical scatterers.

Table 3: NDoF for the 3D scattering experiment

	σ_h	$\hat{\sigma}_{\mathbf{n},h}$	u_h	\hat{u}_h
NDoFs	56 994 735	16 616 295	18 998 245	16 616 295

on the left boundary. For the discrete space, a polynomial degree of $p = 4$ has been used and the maximal mesh size was chosen as $h = 2\pi/2\kappa$. The simulation has been carried out on 16 cores, required approximately 153 GB of memory and the NDoF can be seen in Table 3. The solver stopped after 417 iterations with a wall time of 8204 s.

Acknowledgment

The authors are grateful to Jens Markus Melenk for the informative discussions on the topic of the paper, especially, for pointing out the wave number dependency of the adjoint Helmholtz problem. This work was supported by the "University SAL Labs" initiative of Silicon Austria Labs (SAL) and its Austrian partner universities for applied fundamental research for electronic-based systems and the authors acknowledge the support of Bernhard Auinger of SAL.

References

- [CGS10] Bernardo Cockburn, Jayadeep Gopalakrishnan, and Francisco-Javier Sayas. A projection-based error analysis of HDG methods. *Mathematics of Computation*, 79(271):1351–1367, 2010.
- [DGMZ12] Leszek Demkowicz, Jayadeep Gopalakrishnan, Ignacio Muga, and Jeff Zitelli. Wavenumber explicit analysis of a DPG method for the multidimensional Helmholtz equation. *Computer Methods in Applied Mechanics and Engineering*, 213:126–138, 2012.
- [FLX16] Xiaobing Feng, Peipei Lu, and Xuejun Xu. A Hybridizable Discontinuous Galerkin Method for the Time-Harmonic Maxwell Equations with High Wave Number. *Computational Methods in Applied Mathematics*, 16(3):429–445, 2016.
- [FW09] Xiaobing Feng and Haijun Wu. Discontinuous Galerkin methods for the Helmholtz equation with large wave number. *SIAM Journal on Numerical Analysis*, 47(4):2872–2896, 2009.
- [FW11] Xiaobing Feng and Haijun Wu. hp-Discontinuous Galerkin methods for the Helmholtz equation with large wave number. *Mathematics of Computation*, 80:1997–2024, 02 2011.
- [FX13] Xiaobing Feng and Yulong Xing. Absolutely stable local discontinuous Galerkin methods for the Helmholtz equation with large wave number. *Mathematics of Computation*, 82(283):1269–1296, 2013.
- [GGS20] Shihua Gong, Ivan Graham, and Euan A Spence. Domain decomposition preconditioners for high-order discretisations of the heterogeneous Helmholtz equation, 04 2020.
- [GM11] R. Griesmaier and P. Monk. Error Analysis for a Hybridizable Discontinuous Galerkin Method for the Helmholtz Equation. *Journal of Scientific Computing*, 49:291–310, 2011.
- [GMO14] Jayadeep Gopalakrishnan, Ignacio Muga, and Nicole Olivares. Dispersive and dissipative errors in the DPG method with scaled norms for Helmholtz equation. *SIAM Journal on Scientific Computing*, 36(1):A20–A39, 2014.
- [HPS13] M. Huber, A. Pechstein, and J. Schöberl. Hybrid Domain Decomposition Solvers for the Helmholtz and the Time Harmonic Maxwell’s equation. In Randolph Bank, Michael Holst, Olof Widlund, and Jinchao Xu, editors, *Domain Decomposition Methods in Science and Engineering XX*, pages 279–287, Berlin, Heidelberg, 2013. Springer Berlin Heidelberg.
- [HS14] M. Huber and J. Schöberl. Hybrid Domain Decomposition Solvers for the Helmholtz Equation. In Jocelyne Erhel, Martin J. Gander, Laurence Halpern, Géraldine Pichot, Taoufik Sassi, and Olof Widlund, editors, *Domain Decomposition Methods in Science and Engineering XXI*, pages 351–358, Cham, 2014. Springer International Publishing.
- [Hub13] M. Huber. *Hybrid discontinuous Galerkin methods for the wave equation*. PhD thesis, Technische Universität Wien, 2013.
- [LCQ17] Peipei Lu, Huangxin Chen, and Weifeng Qiu. An absolutely stable hp-HDG method for the time-harmonic Maxwell equations with high wave number. *Mathematics of Computation*, 86(306):pp. 1553–1577, 2017.

- [Mel95] J.M. Melenk. *On Generalized Finite Element Methods*. PhD thesis, University of Maryland at College Park, 1995.
- [MPS13] J.M. Melenk, A. Parsania, and Stefan Sauter. General DG-Methods for Highly Indefinite Helmholtz Problems. *Journal of Scientific Computing*, 57, 12 2013.
- [MS14] Andrea Moiola and Euan A Spence. Is the Helmholtz equation really sign-indefinite? *Siam Review*, 56(2):274–312, 2014.
- [MSS10] P. Monk, J. Schöberl, and Astrid Sinwel. Hybridizing Raviart-Thomas Elements for the Helmholtz Equation. *Electromagnetics*, 30:149 – 176, 2010.
- [Say13] Francisco-Javier Sayas. From Raviart-Thomas to HDG: a personal voyage. 2013.
- [Sch97] J. Schöberl. NETGEN An advancing front 2D/3D-mesh generator based on abstract rules. *Computing and Visualization in Science*, 1:41–52, 07 1997.
- [Sch14] J. Schöberl. C++11 Implementation of Finite Elements in NGSolve, 09 2014.
- [SZ05] J. Schöberl and S. Zaglmayr. High order Nédélec elements with local complete sequence properties. *COMPEL*, 24(2):374–384, 2005.
- [Wu14] Haijun Wu. Pre-asymptotic error analysis of CIP-FEM and FEM for the Helmholtz equation with high wave number. Part I: linear version. *IMA Journal of Numerical Analysis*, 34(3):1266–1288, 2014.